

UNIVERSITY OF TARTU

Faculty of Science and Technology

Institute of Physics

Computer Engineering

Georgi Olentšenko

PROTOTYPE DESIGN OF ESTCUBE-2
ATTITUDE AND ORBIT CONTROL SYSTEM

Master's Thesis

Supervisors:

M.Sc. Andris Slavinskis

M.Sc. Viljo Allik

Tartu 2014

Contents

Acronyms and Abbreviations.....	4
1 Introduction.....	5
2 Overview.....	6
2.1 ESTCube-1.....	6
2.2 ESTCube-2 and ESTCube-3 Missions.....	6
2.3 Overview of Attitude and Orbit Control Systems.....	8
3 ESTCube-2 Attitude and Orbit Control System.....	10
3.1 Requirements.....	10
3.2 System Structure.....	11
3.2.1 Sensors.....	12
3.2.2 Thrusters and Torquers.....	13
3.2.3 Management Hardware.....	13
4 Prototype Design.....	14
4.1 Requirements.....	15
4.2 Concept.....	16
4.3 Hardware Selection.....	18
4.3.1 Processing Unit.....	18
4.3.2 Gyroscopic Sensors.....	20
4.3.3 Magnetometers.....	21
4.3.4 Accelerometers.....	21
4.3.5 Analog-to-Digital Converters.....	23
4.3.6 Power Management Hardware.....	24
4.3.7 Debugging Functionality.....	24
4.4 Prototype Board Design.....	25
4.4.1 Schematic.....	25
4.4.2 Board Layout.....	29
4.4.3 Result.....	32

4.5 AOCS Prototype Analysis and Firmware Development.....	32
5 Summary.....	34
6 Acknowledgements.....	35
Kokkuvõte.....	36
References.....	37
Appendices.....	43
Appendix A – Prototype Board Schematic.....	43
Sensors group.....	43
ADCs group.....	45
Power management group.....	47
MCU group.....	52
Debugging group.....	55
Connector group.....	57
Appendix B – AOCS Prototype Board Layout (Full scale).....	59
Appendix C – Prototype Board Bill of Materials.....	62
Appendix D – Board Layout Design Strategy.....	65

Acronyms and Abbreviations

CG	Cold Gas
AOCS	Attitude and Orbit Control System
OBC	On-Board Computer
EPS	Electric Power System
LEO	Low Earth Orbit
ADCS	Attitude Determination and Control System
CDHS	Command and Data Handling System
PWM	Pulse Width Modulation
ADC	Analog-to-Digital Converter
COTS	Commercial Off-The-Shelf
GPS	Global Positioning System
MCU	MicroController Unit
FPU	Floating-Point Unit
dps	degrees per second
UART	Universal Asynchronous Receiver/Transmitter
USART	Universal Synchronous/Asynchronous Receiver/Transmitter
SPI	Serial Peripheral Interface
IC	Inter-Integrated Circuit
FRAM	Ferroelectric Random Access Memory
SRAM	Static random-access memory
LSB	Least Significant Bit
I/O	Input Output
kSPS	kilo Samples Per Second
PCB	Printed Circuit Board
CAD	Computer-Aided Design
RMS	Root Mean Square
IC	Integrated Circuit
LDO	Low-Dropout Regulator
RTC	Real Time Clock
LED	Light-Emitting Diode

1 Introduction

The CubeSat standard [1] popularity has drastically risen over the last few years. It is a great opportunity for universities to get their students involved in space technologies as well as to allow cost effective space experiments for scientists and companies. Some examples of in-orbit experiments include COMPASS-1 [2], STRaND-1 [3], Aalto-1 [4], SwissCube [5] and RAX [6], all of which have various objectives. Estonian students joined the movement with ESTCube-1 satellite [7]. The main scientific mission of the satellite is to test the electric solar wind sail (E-sail) invented by Pekka Janhunen [8].

E-sail is a propellantless propulsion method, which is achieved by extracting momentum from solar wind protons [9]. The protons are repelled by a long conducting tether, which is kept at high positive potential with the help of an electron gun [10].

The first Estonian satellite was successfully developed and launched by the effort of over a 100 students and instructors from different countries [11]. Although the main experiment is yet to be performed and the work continues, the next missions are already being planned and analyzed. In particular ESTCube-2 and ESTCube-3 missions intended to test the E-sail further as well as to demonstrate the NanoSpace Cold Gas (CG) thrusters [12], both of which could be viable transportation methods in space [13].

This work concentrates on the development of the first prototype of the Attitude and Orbit Control System (AOCS) for ESTCube-2. AOCS is critical for scientific mission success, because it is responsible for E-sail experiment and CG thruster demonstration. The work on ESTCube-1 has given enormous amount of experience to the ESTCube team, hence the best features of ESTCube-1 Attitude Determination and Control System (ADCS) will be reused and known flaws will be corrected. Nevertheless, new technologies will also be tested using the AOCS prototype.

The main goals of this work were stated as follows:

- specify the requirements for the Attitude and Orbit Control System of ESTCube-2 satellite;
- describe the structure of ESTCube-2 AOCS;
- specify the requirements for AOCS prototype board;
- select hardware for the AOCS prototype main board;
- design the AOCS prototype board.

Full description of assembly and testing of AOCS prototype as well as firmware development is out of the scope of this thesis, but a short-term plan is discussed.

2 Overview

This part of the work describes the missions of Estonian student satellite program as well as gives a brief overview of other nanosatellites, which implemented attitude and orbit control systems. Section 2.1 reviews the ESTCube-1 mission in slightly more detail. Section 2.2 introduces the future ESTCube missions. Section 2.3 analyzes the attitude and orbit control systems of nanosatellite projects.

2.1 *ESTCube-1*

ESTCube-1 is the first project of the Estonian student satellite program [11]. The main objective of the program as a whole is to promote space technology and give students a hands-on experience in building a space craft. The main scientific objective is to demonstrate the electric solar wind sail (E-sail). During the experiment the satellite will be spun up to 360 deg/s, at which point a 10 m long aluminium tether will be reeled out with the help of the centrifugal force [7]. Afterwards the tether will be charged to 500 V potential. E-Sail force will be determined by the change of satellite attitude and the measurements of tether current [14].

ESTCube-1 – Estonia's first satellite was developed over a period of five years and has been launched on May 7, 2013 on-board Vega VV02 rocket to Low Earth Orbit (LEO). After the launch all satellite systems were verified to be fully operational with the exception of some minor issues. During the following year the on-board firmware development continued. As of May 27, 2014 preparations for the scientific mission are still in progress. Nevertheless Estonian student satellite program has already fulfilled many of its objectives with the launch of ESTCube-1. [7]

2.2 *ESTCube-2 and ESTCube-3 Missions*

Based on the success of the first satellite, the ESTCube team has started planning more missions. Although the main scientific experiment of ESTCube-1 mission has not been performed yet, future plans include testing the longest yet tether (1 km) for the electric sail experiment and utilizing a miniaturized microelectromechanical systems (MEMS) based cold gas (CG) thruster for attitude and orbit control [12]. Main purpose of ESTCube-2 and ESTCube-3 missions is to demonstrate the technologies.

Both propulsion technologies could be used by lightweight spacecrafts for exploration. These technologies could possibly allow access to any asteroids (i.e. asteroid mining), multi-asteroid touring without additional propellant cost and asteroid deflection for protection of Earth. [15]

Satellite structure and objectives of both missions are very similar and the main difference is in the target orbit. ESTCube-3 mission will take place on highly elliptical Earth or lunar orbit, both of which provide solar wind environment and a reduced influence of Earth's magnetic field. Unfortunately such orbit launches are not frequent, so it is possible that ESTCube-3 mission will have to wait until such launch is available. The main objective of ESTCube-2 mission is to test the hardware and firmware for the ESTCube-3 mission on the low Earth orbit, which is more easily accessible and the risk of mission failure is decreased.

In this work mainly ESTCube-2 mission will be discussed, but in most cases both missions are applicable.

Although ESTCube-1 created a baseline for ESTCube future missions, ESTCube-2 tasks require significantly more hardware and processing power. Figure 1 shows the first model of ESTCube-2. The satellite is a 3-U CubeSat ($300 \times 100 \times 100$ mm, 4 kg), which is three times larger than ESTCube-1. The two main payloads are located at the opposite ends of the satellite. The rest of the hardware will be placed in between the payloads.

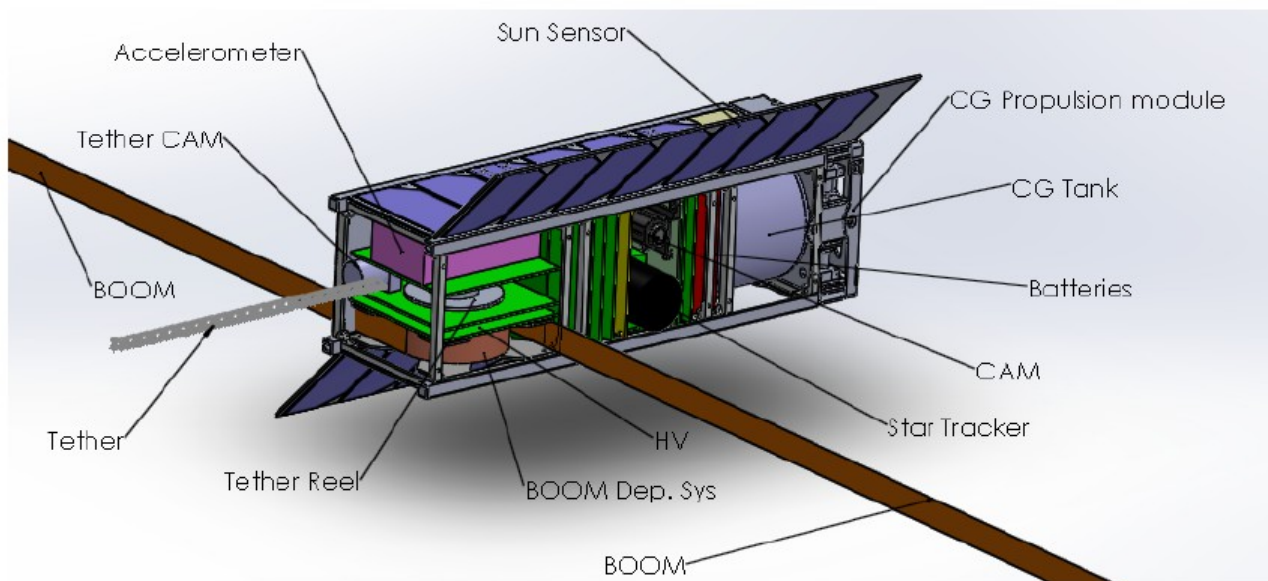


Figure 1: First ESTCube-2 model by Paul Liias (PL Space OÜ).

One kilometer tether weights 11 g and was proved to be automatically producible [16]. It will be reeled out by a motor, design of which will be similar to ESTCube-1 and Aalto-1 missions. A camera will verify the reeling. High Voltage (HV) system will provide the tether with the required +10 kV potential. Deployable fixed booms will be used to study the effect of electron chaotisation [17]. An electron gun should also be on the satellite, although it is missing from the

model.

NanoSpace Cold Gas propulsion base module is $100 \times 100 \times 30$ mm in size and has an interface board on top of it. Module includes four thrusters facing the same direction to maximize possible propulsion force. The module contains 50 g of butane, which should provide a total of 40 Ns of impulse for the mission [19]. The CG tank in Figure 1 model indicates that the module could be increased in size to allow a larger amount of butane on board. The exact required amount of propellant will be calculated in later stages of development.

Deployable solar panels with corresponding attitude control would allow the power production to increase. Star tracker is the main and most accurate attitude sensor on satellite board. Sun sensors are less accurate attitude sensors, but they allow more frequent measurements. Camera subsystem will be used to take images of the nearby space objects of interest. The satellite also includes electric power, on-board computer, attitude and orbit control and communication subsystems among others, which are not highlighted on the drawing.

ESTCube-2 should also have back-up systems, which are known to work in LEO. That includes magnetometers and magnetic coils, which have no use outside of the Earth's magnetic field during ESTCube-3 mission.

2.3 Overview of Attitude and Orbit Control Systems

This section will concentrate on hardware solutions of different CubeSat attitude and orbit control systems. In most cases detailed information about the satellites is not published, but general information about the subsystems can still be acquired.

Since ESTCube-2 AOCS is based on ESTCube-1 ADCS [19], it is prudent to start the description from the latter. ADCS uses 2-axis custom made Sun sensors, COTS 3-axis digital gyroscopes and magnetometers to determine the attitude of the satellite. Sensor redundancy is provided by using duplicated sensors connected by separate communication buses. Attitude is controlled solely using magnetic coils in the Earth's magnetic field [20]. Command and Data Handling System (CDHS) also provides cold redundancy for STM32F103 processor [21], which controls the sensors and coils of ADCS. The system proved to be stable, but some issues still exist. For example inability to turn off ADCS sensors independently leads to a need to restart the whole subsystem, if I²C communication to one of the sensors fails.

COMPASS-1 CubeSat was launched in 2008 with objectives of taking images of Earth and testing a GPS receiver from German Aerospace Center (DLR). On-board ADCS used Sun sensors and

magnetometers for attitude determination and magnetic coils for attitude control. ADCS used 8051 and HCS12 microcontrollers. After the launch misalignment of magnetic field reference vector and inaccurate calibration of sun sensors made attitude determination unreliable. [2]

SwissCube was build for educational purposes. Its ADCS uses 3-axis HMC1043 magnetometer from Honeywell, three 1-axis gyroscopes and six novel Sun sensors to determine the Sun vector. Magnetic torquers were used for attitude control [5]. First two years gyroscopic sensors were in saturation and after three years 2 of 12 sun sensors failed. The calibration of the magnetometer was also off in one axis and there occurred I²C communication problems similar to ESTCube-1. In other respects the system worked fine. [22]

CanX-4/-5 satellites were launched to demonstrate formation flying. Satellites are 20 × 20 × 20 cm in size, but still count towards nanosatellite with mass less that 7 kg. Attitude of the satellites was determined by six coarse/fine Sun sensors, a 3-axis magnetometer and three gyroscopic sensors. Satellites were controlled by 3 orthogonally-mounted reaction wheels, 3 magnetorquers and Canadian Nanosatellite Advanced Propulsion System which provides up to 10 mN force per thruster and includes four thrusters. Performance of the system resulted in attitude determination with accuracy of 1° and pointing accuracy of 5°. [23]

UKube-1 has an Active Magnetic Attitude Control subsystem, which has been developed by Clyde Space [24]. Actuation is provided by 6 magnetic torquers and a permanent magnet. Sensing is done by MEMS Inertial and Magnetic Measurement Unit consisting of gyroscopic sensors, accelerometers, magnetometers and coarse Sun sensors. The subsystem is targeting a 2-axis pointing capability of ±5° and sensing accuracy of ±1° [25]. The satellite is scheduled for Soyuz launch on June 19, 2014 [26].

Design of UWE satellite series is continuously improved by the University of Würzburg. Three satellites have already been launched and the UWE-4 with an AOCS is already under development [27]. UWE-3 has been launched on November 21, 2013. Its main purpose is to demonstrate the low power ADCS and its control algorithms. ADCS uses MSP430 processor and three types of sensors: magnetometers, Sun sensors and gyroscopes. Attitude control is achieved by 6 magnetic torquers and a single reaction wheel for fast attitude changes. The satellite exhibits good health after 3 months in orbit, but to improve system performance sensor calibrations and noise factor adjustments must be performed. [28]

One of the main scientific purposes of Aalto-1 satellite is to test a 100 m E-sail tether, although in this case it will be used as a plasma brake [29]. Aalto-1 will use iADCS-100, which is developed by

Berlin Space Technologies and based on TUBSAT platform [30]. It consists of magnetic torquers, magnetometers, accelerometers, gyroscopic sensors, reaction wheels, Sun sensors and a star tracker for accurate attitude control. The platform is still under development. Although Aalto-1 attitude determination and control system is the closest to the one under development for the future ESTCube missions, it lacks orbit control capability in form of propulsion.

From solution reviews one should conclude that the development of attitude and orbit control is not a trivial task and there is no universal solution for every case. Furthermore there is no educational value in buying a ready solution. For those reason it was decided to build a custom made AOCS for ESTCube-2. Additionally it must be noted that the most often occurred problem on all satellites is inaccurate sensor calibrations and insufficient tests. Therefore a prototype with easy testing capabilities should be developed for ESTCube-2 mission.

3 ESTCube-2 Attitude and Orbit Control System

AOCS is critical for fulfilling the scientific mission of the satellite. This part of the thesis describes the AOCS as a whole. Section 3.1 states the AOCS requirements. Section 3.2 describes the structure of AOCS, which fulfills the requirements.

3.1 Requirements

The system is required to perform the following tasks.

- **Pointing** is the most fundamental attitude control task. It must be used to fulfill all of the following tasks in the list as well as pointing antennas for communication with Earth, pointing the solar panels towards the Sun to increase their efficiency and pointing camera for imaging space objects.
- **Spin-up** is required to measure the E-sail effect. It must be achieved by using reaction wheels and magnetic coils in the case of ESTCube-2.
- **Delta-v maneuvers** mean changing the orbit velocity of the satellite, which allows changing the satellite trajectory. Maneuvers will demonstrate the capabilities of CG propulsion module. At the moment it is planned to have all four thrusters of the propulsion module to face in one direction, so pointing is essential for the maneuvers.
- **E-sail effect measurement** should be performed in several different ways to produce reliable results. Measuring and analyzing the change of satellite attitude is one of the methods. Second method implies using a high accuracy on-board accelerometer. Radio

communication based precise orbit determination is the third method.

Following are the estimated accuracy requirements.

- Attitude determination accuracy: **0.5 deg.**
- Attitude control accuracy: **3 deg.**
- Attitude control accuracy of the spin plane: **3 deg.**
- Acceleration measurement accuracy: **3 μ g.**

These requirements drive the AOCS design, which is described in the following section.

3.2 System Structure

This section lists all of the Attitude and Orbit Control Systems components. Structure of the system is based on analysis of previously flown nanosatellites as well as ESTCube-1 and Aalto-1 experience.

A single PCB cannot contain all of the features needed for attitude and orbit determination and control. Therefore full functionality description must include other subsystems and payload hardware, which acts either as a source of information or a way of controlling the satellite. Figure 2 gives an overview of the components without explicit connections. Components are functionally divided into three groups: sensing, actuating and management hardware.

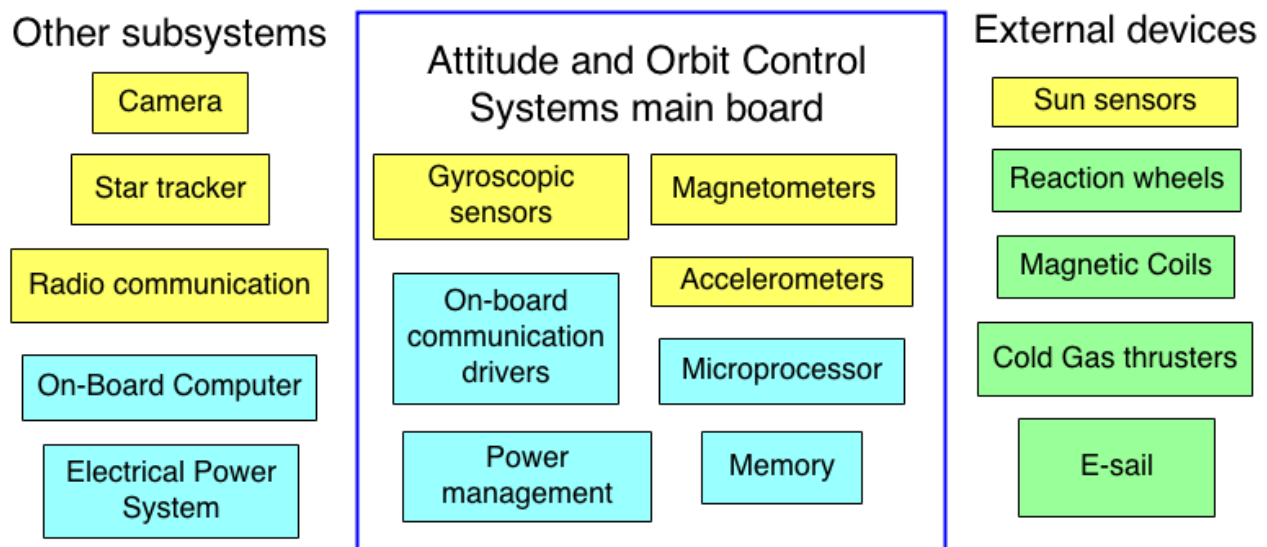


Figure 2: Attitude and Orbit Control Systems components: yellow – sensing, light blue – management, green – actuation hardware.

The following subsection describe the hardware in more detail.

3.2.1 Sensors

- **Star tracker** is the main attitude sensor on ESTCube-2. It is a separate subsystem, containing a monochrome camera and a microprocessor to process the image data. Star tracker determines the attitude by identifying and tracking star formations. Attitude determination with a star tracker is very accurate, but it is limited by the imaging sensor speed and sensitivity, processing power of the system and pointing direction of the imaging sensor. Typically star tracker is too slow to solely rely on it. Moreover usually star tracker is unable to determine attitude, when the satellite rotation is faster than several tenths of degrees per second. E-sail experiment requires a spin-up to 1 rotation per second. Therefore the star tracker must be supported by other sensors that allow higher spin rates. A dedicated connector to AOCS main board is needed, but the communication standard is not yet known.
- **Sun sensors** allow performing attitude determination with less accuracy than star tracker, but measurement results can be acquired more frequently and with greater spinning rate. These sensor allow determining the position of the Sun relative to the satellite. Similarly to ESTCube-1 it is planned to have one sun sensor per satellite side. Each sun sensors should have a separate connector to the AOCS main board. It is not yet determined, whether ESTCube-1 sensors will be reused, or a new digital Sun sensor will be developed.
- **Magnetometers** are used for attitude sensing in LEO. Magnetometers are essential attitude determination sensors on ESTCube-1. On ESTCube-2 it will be used as back-up sensors and for verifying the satellite attitude, because magnetometers cannot be used for attitude determination during ESTCube-3 mission. Magnetometers are placed on the AOCS main board.
- **Gyroscopic sensors** allow determining the spin rate of the satellite. It allows more accurate attitude determination in combination with above discussed sensors. Gyroscopic sensors are placed on the AOCS main board.
- **Accelerometers** are mainly used to measure satellite propulsion methods, but they can possibly used as additional source of information in AOCS algorithms. Small low cost accelerometers will be placed on the AOCS main board to measure acceleration produced by the Cold Gas thruster. Because the E-sail acceleration is too small to measure with such accelerometers instantaneously, a separate high accuracy accelerometer will be placed in the satellite payload. It requires a dedicated connector, but the communication interface is unknown at the moment.

- **Camera subsystem** can be used for attitude verification, but it is not the main purpose of the subsystem. Most likely verification will not be performed on board of the satellite. A dedicated connector to AOCS main board is not needed.
- **Communication system** is used to receive orbit position information from Earth. Most likely the orbit information will pass through the on-board computer, so a dedicated connector to the AOCS main board is not needed.

3.2.2 Thrusters and Torquers

- **Reaction wheels** are the main attitude control actuators. They will be placed in the payload section and must be provided with a dedicated interface to AOCS main board. Currently reaction wheels from Berlin Space Technologies are considered, which prefer I²C at 3.3 V logic level for communication, although several other communication standards could be used.
- **Cold Gas thruster** is used to control the attitude and adjust the orbit of the satellite. The thruster is a complete system located in the payload and requires a separate connector on the AOCS main board. One of the objectives of the missions is to demonstrate the NanoSpace Cold Gas thruster. The interface consists of two I²C connections at 3.3 V logic level and a 5 V power supply.
- **Magnetic coils** are used on ESTCube-1 to control the attitude of the satellite. These will be used as a back-up to reaction wheels on board ESTCube-2 mission because it will still take place in the Earth's magnetic field. ESTCube-3 mission will not include magnetic coils. Although magnetic coil driver will be located on the Electric Power System (EPS), it should be controlled by the AOCS. Control signals include Enable, Direction and PWM signals.
- **E-sail** can also be counted towards AOCS, although the main objective of the missions is to test it. E-sail is the largest payload on board ESTCube-2. Prototype board developed in this thesis does not include the E-sail interfaces.

3.2.3 Management Hardware

- **MCU** controls the whole AOCS. MCU requires sufficient processing power to collect and process all of the attitude and orbit information, as well as control the actuators and propulsion modules. It is a critical part of the system and requires redundancy.
- **External memory** is also needed, because typically internal memory of the MCU is not

sufficient for all of the AOCS information. Moreover internal memory typically consists of flash memories, which are susceptible to radiation induced errors. Therefore external memories with more tolerance towards radiation (like FRAM) must be used.

- **Power management** is required for AOCS, although Electric Power System (EPS) provides the power. This is due to AOCS requirement to turn off all sensors independently, which must be controlled by AOCS itself. Power management includes power and bus switches placed on the AOCS main board.
- **Communication interface hardware.** Although the MCU should have most of the communication drivers that are required for communication with external hardware. Satellite common bus for example uses RS-485 communication, which typically is not supported by a MCU.
- **On-Board Computer** will manage the the AOCS firmware versions as well as buffer the information between AOCS and Communication subsystem. These tasks require high bandwidth communication. Due to that, a dedicated interface is needed. OBC team proposed using a SPI communication.
- **Electric Power System** provides power for the whole satellite, including AOCS. Furthermore AOCS microprocessor is switched by EPS, providing cold redundancy.

4 Prototype Design

Prototype board is designed to allow further development of AOCS. That requires using integrated circuits expected to be used during the mission as well as providing sufficient hardware firmware debugging functionality. Figure 3 gives a simplified overview of above mentioned AOCS prototype board hardware.

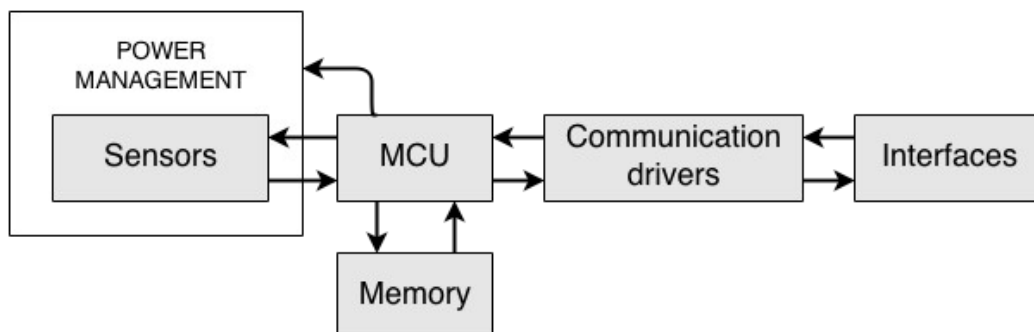


Figure 3: Simplified structure of AOCS prototype board hardware.

Before starting the prototype design, the actual hardware must be selected which is one of the main tasks of this thesis. Section 4.1 lists all explicit requirements for the prototype board and the hardware, which will be placed on the prototype board. Section 4.2 introduces the main concept of the prototype board. Section 4.3 covers the hardware selection. Section 4.4 focuses on the prototype design itself.

4.1 Requirements

Requirements are divided into two groups. One describes general requirements for board design and the second covers the explicit requirements for integrated circuits, that are used in the AOCS prototype design.

- **Allow independently turning off sensors and ADCs.** As mentioned in section 2.3, if ESTCube-1 microprocessor loses communication with a sensor, the only way to reestablish it is to power recycle the subsystem. Although loss of communication with sensors does not occur often, it disturbs control algorithm executions, so ESTCube-2 AOCS design should be improved in respect to that flaw.
- **Provide redundancy for sensors and ADCs.** Several redundancy concepts should be considered and the best one selected and tested on the prototype board, because sensor redundancy is very important in space missions. MCU redundancy is also required on the engineering model of the system, but the design used by ESTCube-1 CDHS has been proven to be sufficient for a 1 year mission. Due to that, MCU redundancy is not implemented on the first prototype board.
- **Allow testing of a range of sensors and ADCs** to determine the best suitable sensor among a number of sensors with very similar properties according to the data sheet. According to the previous requirement redundancy is needed, but different sensors and ADCs could be used.
- **Provide interrupt capability for sensor and ADCs.** Although this requires more communication lines from the MCU, dedicated interrupt lines simplify firmware development. ESTCube-1 firmware is based on delays and timings, which occasionally produce incorrect measurement results due to incomplete conversions.
- **Provide interfaces to different AOCS hardware components for evaluation.** Several components of the AOCS cannot be placed on the AOCS main board because of their size, thus hardware will be placed as payload and requires dedicated interfaces. A range of interfaces (UART, SPI, I²C, RS-485) should be provided by the board.

- **Provide on-board debugging functionality for communication buses.** This functionality will allow simulating hardware by a computer and to verify communication with on-board hardware.
- **Provide temperature and voltage measurements for all sensors and ADCs.** Measuring the temperature and power supply voltage of all sensors would decrease the uncertainties of the sensor measurement results.
- **Provide ability to work from a battery.** Sensor tests, which take place in an confined spaces (i.e. vacuum chamber, temperature chamber) does not allow using a stationary power supply. An on-board battery support would simplify test conduction.

There are explicit requirements for certain AOCS hardware, but other parameters of the hardware are discussed in the corresponding hardware selection subsections.

- **MCU must include a FPU.** Algorithms like Kalman filter require floating number processing. Although they can be done without a dedicated FPU (like on ESTCube-1), its availability would simplify firmware development as well as improve processing time.
- **MCU must provide at least 2 UART, 2 I²C and 3 SPI interfaces** to satisfy sensor and ADC redundancy and provide additional interfaces for external hardware.
- **Gyroscopic sensor sensitivity:** ≥ 100 LSB/dps (resolution ≤ 0.01 dps/LSB).
- **Gyroscopic sensor full range:** ≥ 1800 dps.
- **Magnetometers resolution:** ≤ 80 nT/LSB.
- **Magnetometers full range:** ≥ 0.2 mT.

4.2 *Prototype Board Concept*

The main new concept of the prototype board allows turning off all sensors and ADCs independently. This section first describes the ADCS structure of ESTCube-1 and then explains, how the structure has been improved in ESTCube-2 AOCS to implements the mentioned feature.

Figure 4 shows a simplified structure of ESTCube-1 ADCS. Generalized digital and analog ADCS sensor configuration is shown on the diagram. These sensors are controlled by CDHS microprocessor and powered by EPS. CDHS and EPS provide cold redundancy for the microprocessor with the use of bus switches. If the active microprocessor stops responding, EPS switches the power source. As mentioned before, to turn off one of the ADCS sensors the whole subsystem must be powered off.

To solve the issue, a double bus switch concept was introduced, which expands the microprocessor redundancy idea and applies it to each sensor.

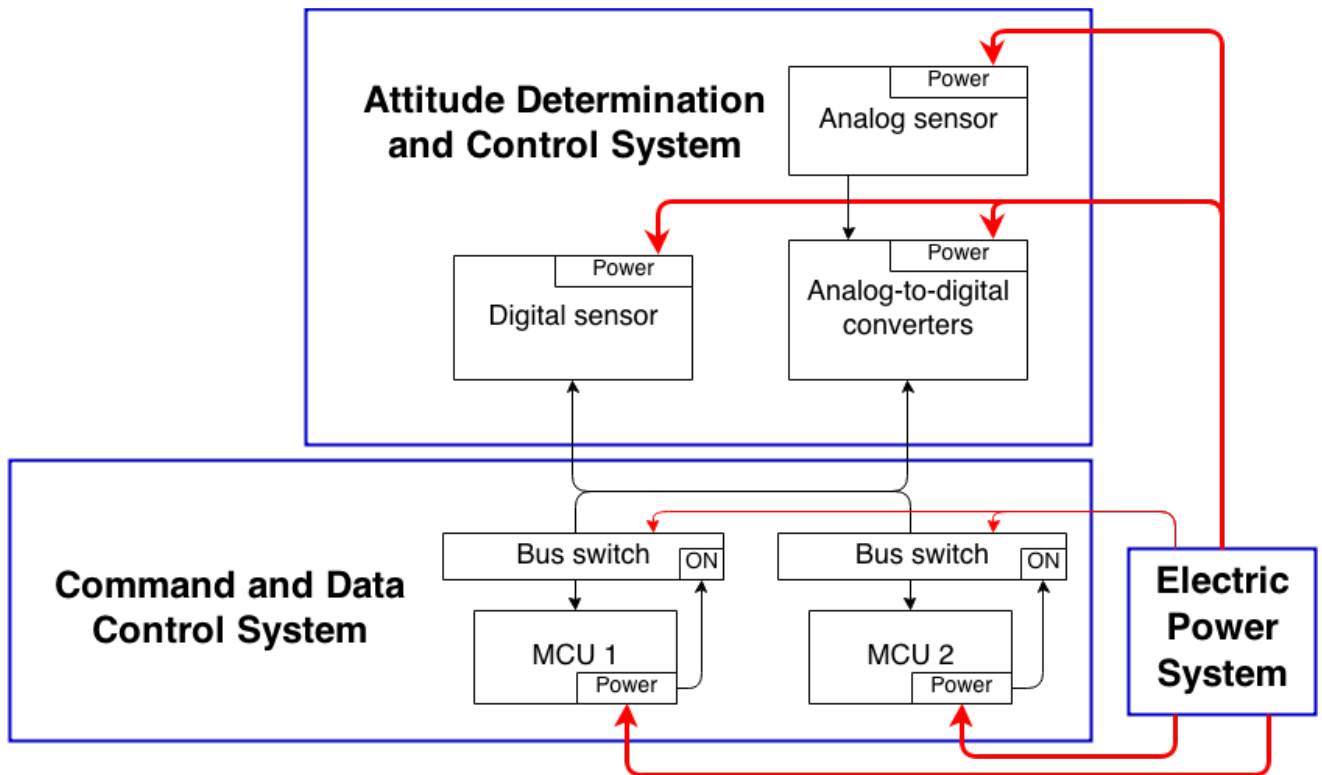


Figure 4: *ESTCube-1 ADCS structure*. Sensors are located on ADCS board, but controlled by CDHS microprocessor. Bus switches are used to provide cold redundancy for the microprocessor. Both systems are powered by Electric Power System.

Figure 5 shows the ESTCube-2 AOCS double switch concept. Each sensor and ADC is supported by a power switch and a bus switch, which isolate the dedicated integrated circuits from power lines and communication bus. The switches are controlled by an I/O expander, so if the microprocessor is switched, the sensors remain in the same state. In contrast to ESTCube-1 ADCS, new concept places the microprocessor on the AOCS main board, but the the same CDHS cold redundancy applies. The concept complicates power management of the board, but it allows to power down sensors and ADCs independently besides sensor redundancy.

The microprocessor redundancy has been proven successful during ESTCube-1 mission, thus the first AOCS prototype contains only one microprocessor. Nevertheless, the double switch concept still applies, because only the bus switches dedicated to the second MCU are removed.

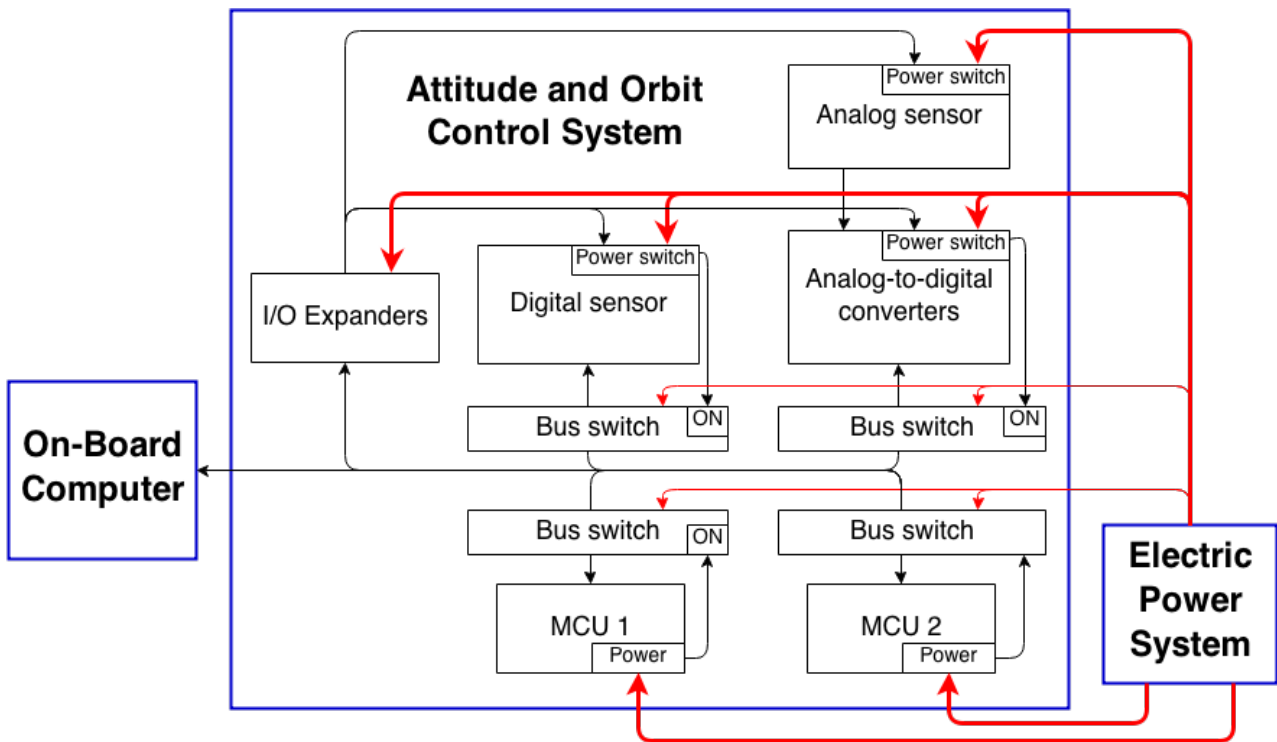


Figure 5: **Double switch concept used in ESTCube-2 AOCS development.** An additional layer of bus switches and power switches provides the functionality of independently turning off the sensors and ADCs.

4.3 Hardware Selection

Hardware selection is one of the main tasks of a prototype design. Availability and price must be taken into consideration in addition to requirement fulfillment. All prices found in the following subsections were referenced from Farnell and EU Mouser (usual ESTCube suppliers) before April 24, 2014. All selected hardware has low mass and small packages.

4.3.1 Processing Unit

ESTCube-1 ADCS does not have a dedicated processing unit, so calculations are run by CDHS STM32F103 microprocessor. Such design simplifies structure of ADCS, lowers power consumption of both systems and eliminates the need of communication between two subsystems. Even so this design also limits the capabilities of both subsystems. ADCS and CDHS have substantially different tasks which must be scheduled and executed by one processing unit. The increase in software complexity caused several problems, which delayed significantly both subsystems software development. In addition, by now ESTCube-1 software development team has

reached task scheduling feasibility limit of the real-time operating system. For those reasons it was decided to use a separate processing unit for AOCS in future missions.

Processors like LPC3180 [31] from NXP Semiconductors were considered because of the double-precision FPU, which would increase accuracy of AOCS algorithms. But NXP processor architecture and firmware design process is unfamiliar to ESTCube team, so it was decided to use the familiar architecture of STM32F4 series, which includes a single-precision FPU and has lower power consumption than other microprocessors with a FPU. Other subsystems also plan to use STM32F4 microprocessors, which means that software development time would decrease even further.

STM32F4 series is based on ARM® Cortex™-M4, which operate at maximum of 180 MHz frequency. By using dynamic power scaling feature, power consumption of the processor can be decreased by lowering the clock frequency. Each processor includes a digital signal processor and a FPU. But there are some differences within the series. Table 1 compares AOCS relevant features of three STM32F4 product lines [32].

Table 1: STM32F4 series AOCS relevant feature comparison [32].

STM32F4 product line	Maximum frequency	Current consumption	Memory size	Package pin number	Communication interfaces
STM32F429/439	180 MHz	260 μ A/MHz	512-KB to 2-MB Flash 256-KB SRAM	100 to 216	4x USARTs 4x UARTs 6x SPIs 3x I ² C
STM32F407/417	164 MHz	238 μ A/MHz	512-KB to 1-MB Flash 192-KB SRAM	64 to 144	4x USARTs 3x SPIs 3x I ² C
STM32F401	84 MHz	128 μ A/MHz	128- to 512-KB Flash 96-KB SRAM	49 to 100	3x USARTs 4x SPIs 3x I ² C

Although STM32F429/439 and STM32F407/417 have superior performance because of the maximum operating frequency, the frequency will likely be reduced to lower the power consumption. That is why STM32F401 has an advantage of approximately 2 times less power consumption compared to other product lines. Flash memory size is not of great importance because it is susceptible to radiation induced errors and has to be supported by more reliable external memory like FRAM. SRAM on the other hand is important, but AOCS algorithms do not

need large memory spaces to operate. I/O pin number of the package is of great importance, but in the current design the MCU is supported by I/O expanders, which decrease the required number of I/O pins. From communication interface variety point of view all product lines are feasible, although a bigger SPI number would be preferable because most of the external devices communicate through SPI. STM32F401 line was selected for AOCS prototype mainly because of its power consumption in spite of smaller SRAM and lower SPI number. To support the processor a FM25V20 FRAM [33] and DS3234 RTC [34] have been selected.

4.3.2 Gyroscopic Sensors

ITG-3200 [35] 3-axis gyroscopic sensor from InvenSense was selected for ESTCube-1 mission. Although ESTCube-1 team has successfully used this sensor during the mission, there are two disadvantages of using ITG-3200 sensor in the future. First of all sensitivity of ITG-3200 is lower than the required sensitivity for ESTCube-2/3 missions. Secondly the only possible interface to communicate with the sensor is I²C, which the team had problems with. In particular the sensor cannot be shut down independently because it draws current from I²C bus.

Table 2: Set of gyroscopic sensors selected for testing on AOCS prototype

Gyroscopic sensor	Measurement range (dps)	Sensitivity (digit/dps)	Sampling rate (Hz)	Noise density (dps/ $\sqrt{\text{Hz}}$)	Supply current (mA)	Interface	Price (€)
ITG-3200 [35]	± 2000	15	8000	0.03	6.5	I ² C	21,7
MAX21000 [36]	± 32 to ± 2000	960 to 15	10000	0.009	5.2	SPI/ I ² C	7.2
BMG160 [37]	± 125 to ± 2000	240 to 15	2000	0.014	5	SPI/ I ² C	3.9
MPU-6000 [38]	± 250 to ± 2000	120 to 15	8000	0.005	3.6	SPI/ I ² C	14.9
L3GD20H [39]	± 250 to ± 2000	120 to 15	800	0.011	5	SPI/ I ² C	4.0
LPY403AL[40]/ LPR403AL[41]	± 30 to ± 120	33.3 to 8.3 mV/dps	140	0.01	6.8	Analog	6.0/ 6.8

Table 2 compares ITG-3200 and the new set of sensors that has been selected for testing. MAX2100, BMG160, MPU-6000 and L3GD20H are digital 3-axis gyroscopic sensors. LPY403AL and LPR403AL are analog 2-axis gyroscopic sensors. The measurement range requirement is fulfilled by all sensors excluding LPY403AL/LPR403AL. LPY403AL/LPR403AL are on the list because it was suggested to have different sensors for low and high spin rates as well as to test

feasible analog gyroscopic sensors. At least a 20-bit low noise ADC is required for accurate measurements in the full range of LPY403AL/LPR403AL.

Both sensitivity and noise density of all sensors are satisfying and the sensors consume relatively similar amount of current. All digital sensors have SPI interfaces, which is used in the design. From the price point of view only MPU-6000 is relatively more expensive than other sensors. Excluding ITG-3200 all sensors are included in the AOCS prototype design.

4.3.3 Magnetometers

Magnetometers are less important for future missions because ESTCube-3 mission is planned to take place outside Earth's magnetic field. That is why ESTCube-2 must be fully operational without the use of magnetometers. Nonetheless, magnetometers are meant to be back-up sensors.

Table 3: Set of magnetometers selected for testing on AOCS prototype

Magnetometer	Measurement range (mT)	Resolution (nT/LSb)	Sampling rate (Hz)	Noise density (nT/ $\sqrt{\text{Hz}}$)	Supply current (mA)	Interface	Price (€)
HMC5883L [42]	± 0.1 to ± 0.8	73 to 435	160	200	0.1	I ² C	3.3
LIS3MDL [43]	± 0.4 to ± 1.6	15 to 58	80	320	0.27	SPI/I ² C	2.0
MAG3110 [44]	± 1	100	80	400	0.9	I ² C	1.0
LSM303D [45]	± 0.2 to ± 1.2	8 to 48	100	500	0.3	SPI/I ² C	4.0
FXOS8700CQ[46]	± 1.2	100	1500	100	0.44	SPI/I ² C	2.4

HMC5883L magnetometer was chosen for ESTCube-1 mission, which similarly to gyroscopic sensors has only a I²C interface. Although HMC5883L satisfies the requirements I²C interface use is undesirable, so a new set of sensor was selected for testing, which can be found in Table 3.

HMC5883L, LIS3MDL, MAG3110, LSM303D and FXOS8700CQ are 3-axis low price magnetometers. All sensors fulfill the requirements. In addition, LSM303D and FXOS8700CQ are considered as acceleration sensors in the next section, which makes them more desirable. The only drawback for HMC5883L and MAG3110 is the use of I²C interface. Nevertheless, all listed sensors are used in the design.

4.3.4 Accelerometers

Accelerometers were not included in ESTCube-1 mission. Main purpose of accelerometers on

board ESTCube-2 is to measure the acceleration gained by using the NanoSpace Cold Gas thrusters and E-sail experiment, although they can possibly be used for attitude estimation. CG thruster and E-sail experiment have different measurement accuracy requirements, so they are discussed separately.

Single CG thruster is capable of providing 1 mN of force. Satellite mass is estimated to be 4 kg. There will be 4 thrusters on board, but even a single thrust must be detectable. Calculations ($1 \text{ mN}/4 \text{ kg}=250 \text{ } \mu\text{g}$) show that the selected accelerometer must detect at the least 250 μg of instantaneous acceleration. Such accuracy is rare in low cost accelerometers, because typically measurement noise is very high. Table 4 compares the set of best found accelerometers.

Table 4: Set of accelerometers selected for testing on AOCS prototype

Accelerometer	Measurement range (g)	Sensitivity	Sampling rate (Hz)	Noise density ($\mu\text{g}/\sqrt{\text{Hz}}$)	Supply current (mA)	Interface
LSM303D [45]	± 2 to ± 16	16384 digit/g	1600	150	0.3	SPI/I ² C
FXOS8700CQ [46]	± 2 to ± 8	4096 digit/g	1500	126	0.44	SPI/I ² C
KXR5 [47]	± 2	660 mV/g	1000	45	0.5	Analog

KXR5 3-axis analog accelerometer perfectly satisfies the requirements, but requires at least a 20-bit low noise ADC to be able to provide accurate measurements in the sensors full range. LSM303D is a 3-axis digital accelerometer and also satisfies the requirements, but noise density is relatively high. FXOS8700CQ 3-axis accelerometer resolution is 244 $\mu\text{g}/\text{LSB}$, so it is unlikely that it will be able to detect 250 μg acceleration. Nevertheless, FXOS8700CQ and LSM303D are also in magnetometer test set. All three accelerometers are used in the design.

FXLC95000CL [14] was also considered for the test set, but discarded because of the included 32-bit ColdFire MCU. Another processor would have meant more firmware development on a separate unfamiliar platform. It has similar accuracy to FXOS8700CQ.

Expected E-sail acceleration with 1 km tether, 10 kV power supply and 4 kg satellite is 5 μg . Such acceleration is impossible to measure instantaneously with low cost accelerometers. Several high accuracy accelerometers are considered for E-sail experiment measurements, but none of them fit on the AOCS main board and would be added as satellite payload. In that case a communication interface must reserved for the sensors. Table 5 introduces the most relevant features of two

possible sensors. Both sensors are 1-axis seismic accelerometers. Discussed high accuracy analog accelerometers are still being analyzed and final decision is not made in this thesis.

Table 5: Possible high accuracy accelerometers for E-sail effect measurement

Accelerometer	Package size (mm)	Voltage	Supply current (mA)	Range (g)	Sensitivity (V/g)	Noise density ($\mu\text{g}/\sqrt{\text{Hz}}$)
393B05 [49]	25 × 24 × 32	18 to 30	10	±5	1	0.3
SF1600S.A [50]	25 × 20 × 15	6 to 15	11.7	±3	1.2	0.3

4.3.5 Analog-to-Digital Converters

Analog sensors require low noise ADCs with high precision voltage references, temperature and input voltage measurements. All of these are chosen in this chapter.

12-bit ADCs are required for Sun sensors, temperature and voltage measurements. ESTCube-1 mission included a 16-channel 12-bit MAX1230 [51] ADCs. This ADC is sufficiently accurate and with high sampling rate, but during the research mentioned ADC was practically out of stock from all usual suppliers. For that reason two substitute ADCs were selected for testing: MAX11633 [52] and AD7940 [53]. The main difference of these ICs from MAX1230 is that they operate at 3.3 V and consume slightly less current (2.0 mA and 1.8 mA accordingly compared to 2.8 mA). In addition, AD7940 has sampling frequency of up to 1000 kSPS compared to 300 kSPS of the MAXIM ADCs. Both MAX11633 and AD7940 are included in the design in a duplicating manner.

Measuring analog accelerometer and gyroscopic sensor outputs on the other hand require an ADC with higher resolution. It was calculated that at least 20-bit resolution is needed to provide accurate measurements. Similarly two ADCs were selected for testing: AD7718 [54] and AD7173 [55]. Both are low power and low noise 24-bit ADCs. AD7718 has up to 10 channels and up to 1.365 kSPS. AD7173 has up 16 channels and 31.25 kSPS, but it is new on the market and may contain faults. Both ADCs are used in the design, but AD7173 has more measurement connections because of the greater number of channels.

KTY82 series [56] resistive temperature sensor was used on ESTCube-1. It implies using a voltage divider, so temperature to voltage transition is not linear and has to be recalculated according to the complimentary resistor of the voltage divider. Due to that, a new temperature sensor was selected that would simplify temperature measurements. LMT86 [57] temperature sensor was selected because of its push-pull output, which is within the range of 3 V. LMT86 consumes up to 9 μA and

has a smaller package (SC-70-5) than KTY82 series sensors.

ESTCube-1 used ADR3450 [58] reference voltage, but it was meant for ADCs operating at 5 V level. ADR3430 [58] was selected from the same series, because it provides the best voltage level accuracy with low voltage drop-out (250 mV maximum) and low power consumption (100 μ A). This 3 V voltage reference is used for both 24-bit and 12-bit ADCs.

4.3.6 Power Management Hardware

Main purpose of power management electronics is allow independently turning off ICs or disconnecting them devices from communication buses. This functionality is provided by using power and bus switches. Power switches disconnect the power supply of a device and bus switch isolates communication interface of the same device. The most important devices that have to be provided with this functionality are the sensors and ADCs.

TPS22941 [59] load switch with 40 mA current limit and thermal shutdown was selected. It also has an auto-restart feature, consumes $< 1 \mu$ A in shutdown mode and has a smaller package (SC-70-5) than other power switches with similar features.

Different devices have different number of I/O pins. For that reason a set of three bus switches was selected: 24-bit SN74CBTLV16211 [60], 10-bit SN74CBTLV3384 [61] and 4-bit SN74CBTLV3126 [62]. All three have the smallest package available to minimize the occupied space on the PCB. All bus switches consume up to 10 μ A current and have a 5 Ω switch connection between the ports.

In addition to actual power management electronics, I/O expanders were selected to simplify switching between MCUs and decreasing the number of needed I/O pins. MCP23S17 [63] is a 16-bit I/O expander with current consumption of 1 mA and a SPI interface.

4.3.7 Debugging Functionality

In addition to main functionality, a prototype board requires additional means of debugging hardware as well as software. This includes voltage regulators, because it is not planned to have those on final version of AOCS main board as the power is provided by EPS. Software debugging is provided by different communication bus to USB interfaces.

Several tests have to be executed in an environment, where connecting the board to a power source is not possible. In that case a battery must be used. LM1117IMPX [64] LDO is used to convert battery voltage to 5 V, which is used for Sun sensors and thruster interface. If the board is power by

an USB interface, 5 V LDO is bypassed. LP2992 [65] is then used to convert 5 V to 3.3 V for the rest of electronic devices. Current sensing is provided by LMP8645 [66] current sense amplifier connected to an ADC, which has adjustable gain and is able to measure current on resistors with higher potential than its power supply.

To allow debugging of the most used communication buses of the prototype, USB interfaces were selected. FT200XD [67], FT220XS [68] and FT230XS [69] provide USB interfaces to I²C, SPI and UART buses accordingly.

4.4 Prototype Board Design

This section introduces the AOCS prototype board design concept and describes both schematic and board layout of the prototype. Prototype contains approximately 450 electronic components, which is difficult to maintain without establishing a design structure. Schematic and board design have slightly different logical structure, which will be described in the following subsections.

A free DesignSpark PCB CAD tool was used for both schematic and board layout designs.

4.4.1 Schematic

This section describes schematic of the prototype board and explains placement of additional electronic components. Schematics of the prototype board can be found under Appendix A. Figure 6 shows the general structure of the AOCS prototype board, which contains the selected hardware.

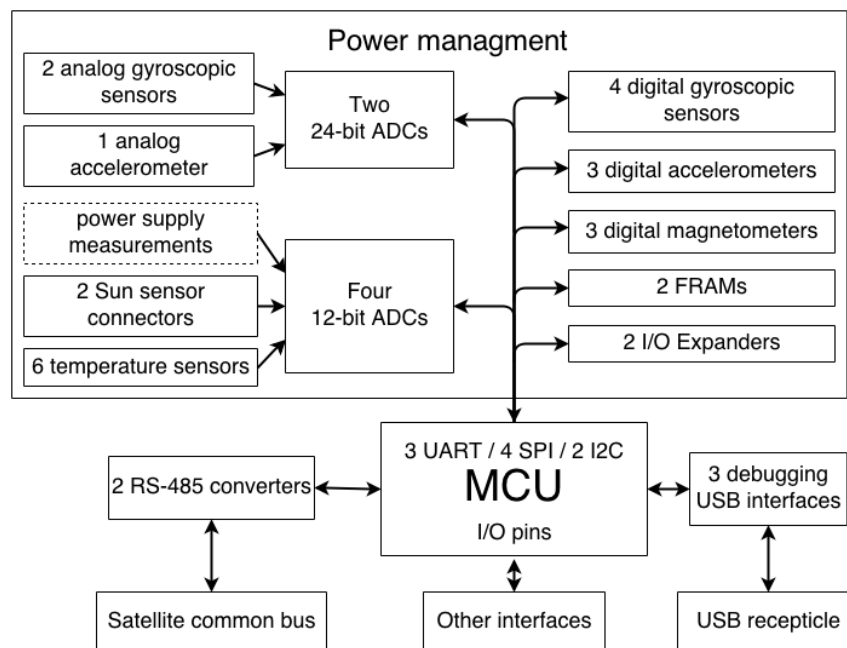


Figure 6: AOCS prototype contents.

The schematic of the prototypes contains almost a hundred integrated circuits each of which requires external electronic components to function stably and lower the noise margin. The schematic is divided into block, where each IC is surrounded by the dedicated signal integrity electronic components.

Even if the main power supply of the board is exceptionally stable, impedance of the traces and other signals throughout the board could influence the stability of an IC power supply. Therefore all ICs in general require decoupling capacitors to reduce input ripple of the power supply. In several cases separate capacitors are used close to analog and digital power supplies of one IC, although the same power supply is used. Typically a 100 nF capacitor is used. In some cases smaller or larger capacitor is needed depending on the integrated circuit.

Communication buses used on the board require pull-up resistors. In particular, I²C needs pull-up resistors on both signal lines and SPI requires a separate pull-up on every chip select signal. Pull-ups are placed next to slave devices to drive the signal high when the processor is not driving the signal. Pull-down resistors are also needed to drive some other signals to low level. These signals include selftest pins for analog sensors for example.

In addition to above described cases, most ICs require external electronic components for other reasons. Those reasons are described separately in each cases during this section. To simplify the structure of the schematic as well as its description, components were divided into 6 functional groups: sensors, ADCs, power management, MCU, debugging and connector groups. Schematic of the prototype can be found under Appendix A in figure 8-24.

1. Sensors group

The group includes four digital and two analog gyroscopic sensors (figure 8), three magnetometers, two digital accelerometers, one analog accelerometer and six temperature sensors (figure 9).

MPU-6000 includes a LDO and a charge pump, which generates high voltage for MEMS oscillators. They require 0.1 μ F and 2.2 nF capacitors accordingly. L3GD20H requires a 10nF filter capacitor. LPR403AL and LPY403AL require a low pass filters for the phase lock loop (PLL) circuit to synchronize driving and sensing circuits.

HMC5883L requires 4.7 μ F reservoir and 0.22 μ F set/reset strap drive capacitors, which are used to handle 1 A peak current pulses. LIS3MDL has a 100 nF capacitor connected to a dedicated C1 pin. MAG3110 needs two 100 nF capacitors for bypassing the internal regulator and magnetic reset pulse circuit.

Bandwidth of KXR5 analog accelerometer is determined by a filter capacitor. A 4.7 nF capacitor allow frequencies of up to 1 kHz. FXOS8700CQ requires two additional 100 nF capacitors for bypassing the internal regulator and for the magnetic reset pulse. It is recommended to connect a 4.7 μ F reservoir and a 0.22 μ F set/reset capacitors to LSM303D sensor.

To reduce the output noise coupling of the LMT86 temperature sensor, a 1 nF capacitor is used.

2. ADCs group

This group includes six ADCs and two voltage references dedicated to the ADCs (figures 10 and 11).

A 1 μ F capacitor is connected to voltage references output to improve stability and reduce the high frequency noise. All ADCs have additional 0.1 μ F capacitors on the reference inputs for the same reason.

Both 24-bit ADCs have separate crystal oscillators, which are higher precision and lower jitter clock sources compared to internal clock sources. AD7173-8 on the other hand has two on-board LDO regulators, both of which require 1 μ F and 0.1 μ F capacitors to the corresponding pins.

Although 12-bit ADCs and AD7718 do not require more external electronic components, in addition to mentioned to the ones described at the beginning of the section. All high precision ADCs require certain layout considerations though, but that is described in the board layout section.

Because 3 V references are used, voltage dividers must be used to bring the the peak voltage of several signals under 3 V. Voltage dividers are used for all sensor power supply voltage measurements and Sun sensor signals, which maximum voltage could be as high as 5 V.

3. Power management group

This group consists of I/O expanders, power switches and bus switches, not dedicated to the MCU (figures 12, 13, 14, 15 and 16). There are 20 power switches in this group. Each one has stabilizing capacitors on input and output and a pull-down resistor on the enable signal to ensure that on start-up the power switch is turned off. In addition to that, all power switches have a single common signal: power fault – an open-drain output, which requires a pull-up resistor. SN74CBTLV3384 bus switches also require inverters to the enable output signals because they are activated at low level. Without inverters bus switch would be activated after start-up.

4. MCU group

This group includes the STM32F4 processor (figure 17), four bus switches (figures 18 and 19), a RTC, two FRAM memories and two RS-485 converters (figure 20).

STM32F4 processor requires two 2.2 μF capacitors for the main on-board regulator and two quartz oscillators: 32 kHz for the internal RTC and 16 MHz as the main clock source. Also one LED is placed next to the MCU for debugging purposes, because the rest of the LEDs is placed behind the bus switches.

SN65HVD75 RS-485 drivers require transient-voltage-suppression diodes, which protect the communication bus from voltage spikes. The value of the resistor between A and B differential signals depends on the impedance of the connection, so at the moment it is left undefined.

5. Debugging functionality group

This group consists of LDOs (figure 21), USB communication drivers for different bus interfaces, current sensing, control buttons and LEDs (figure 22).

LP2992 and LM1117 LDOs have the typical input and output stabilizing capacitors, but LP2992 requires another dedicated bypass 10 nF capacitor. LMP8645 current sense amplifier uses a 0.1 Ω shunt resistor to measure the voltage drop and 50 k Ω resistor, which defines the gain of the amplifier. The current consumed by the whole board is measured.

FT230XS, FT220XS and FT200XD are FTDI USB interfaces require 27 Ω resistors on the USB signal lines to stabilize the signals. Two LEDs were connected to FT230XS ICs, because it will be the main debugging interface and indicators of its activity are needed.

There are five mechanical switches to control the board. Three of the switches are used to control the power of the board. Fourth switch select the boot mode of the processor. Fifth switch resets the processor. All switches have debouncing circuits in form of 10 μF and 100 nF capacitors to make level transitions smoother.

There are 15 LEDs in total on the board. One is part of the MCU group. Two are UART to USB driver indicators. Three LEDs are power indicators. There rest is are debug LEDs connected to either MCU or I/O expanders.

6. Connectors

There are several connectors for different purposes on the board (figures 23 and 24). Some are interfaces to external AOCS hardware like sun sensor connectors, cold gas thruster interface or coil driver interfaces. Others are meant for communication to other subsystems of the satellite like the common bus and OBC interface. There are also two connectors for additional sensors, which are needed in case some sensor is added to the test list at later development stages. There is a battery connector with a rectifier diode to prevent wrong polarity connection of the battery and a jumper,

which is meant to allow connecting USB and battery 5 V source in case power source must be switched without powering down the whole board. And there are of course the debugging interfaces: SWD two-wire interface for STM32F4 debugging and the USB connectors for the USB drivers. USB connectors require 27 pF capacitors for the signal lines to stabilize the communication.

4.4.2 Board Layout

This section describes the concepts involved, strategy used and decisions made during board design for the prototype board. Board design by layer can be found under Appendix B.

A 4 layer board design is used, which allows using a ground plane as one of the layers. A whole layer dedicated to ground provides low ground impedance and allows avoiding ground loops in most cases. This also significantly simplifies the design, because practically each circuit has a ground connection.

Appendix C contains the full bill of materials for AOCs prototype board. Several hundreds of components with about 1500 connections is difficult to organize without a strategy. The design strategy must take into account that certain components have to be placed in certain respect with each other and that there are only 3 layers available for routing, excluding ground plane. Decoupling capacitors for example as well as other signal integrity related components are required to be placed next to the IC dedicated pins. Taking that into consideration the first step of the strategy is to combine components in to groups according to schematic blocks.

Second step is to organize the groups within them selves. Placing external electronics components next to the IC dedicated pins is critical to simplify further organization. At this point similarity of the board layout design to the schematic ends. Result of this step should consist of groups organized on one of the sides of the board.

The third step is to organize the groups into power management units with a single power supply and bus interface. For example a sensor is combined with the dedicated power and bus switches. The outcome of the this step is usually a two side unit with relatively small amount of external connections. At this point some routing could be done, but only on the layers that the components are placed.

The fourth step is to organize these units into the overall structure of the board, taking into consideration communication buses and the main power supply. Separating analog and digital signals is also advised, especially if high accuracy measurements are performed. Usually it takes several tries to get a suitable structure.

After the main structure of the board is established, the last step must be taken: optimization. Optimization means readjusting the components for optimal space and connectivity. Usually unoptimized groups take more space and have intertwined signals in respect to the board structure. Optimization is needed to improve the final composition of the board. The last step typically takes the most time of the board layout design. Visual representation of the strategy can be found under Appendix D.

In addition to general strategy of the board layout design, certain decisions were made to simplify the structure of the board. It was decided to place all of the sensors on the top side of the board and mark the measurement directions with silkscreen. Similarly power management ICs are mostly placed on the bottom of the board. This allows creating the power management units described in the design strategy.

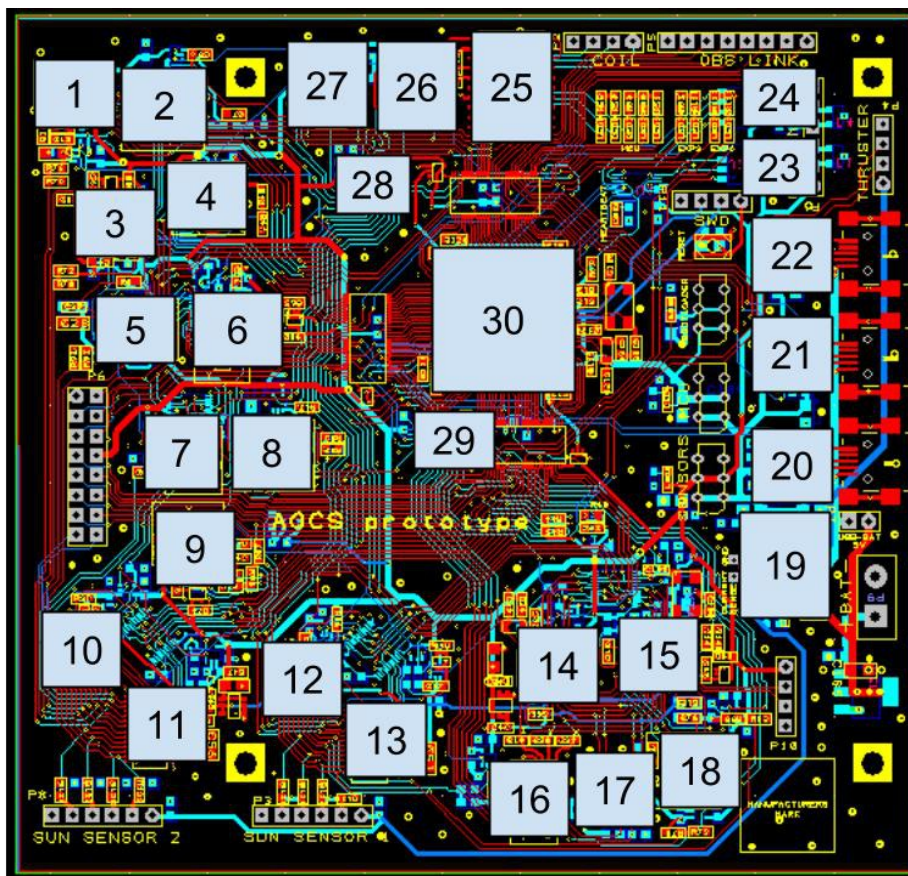


Figure 7: Main ICs of AOCS prototype board. 1-4 – digital gyroscopes. 5-6 – digital accelerometers, 7-9 – magnetometers, 10-13 – 12-bit ADCs, 14-15 – 24-bit ADCs, 16 – analog accelerometer, 17-18 – analog gyroscopes, 19 – 3.3 V LDO, 20-22 – USB interfaces, 23-24 – RS-485 drivers, 25 – RTC, 26-27 – FRAM, 28-29 – I/O Expanders, 30 – MCU.

Figure 7 highlights the main ICs on the prototype excluding power and bus switches. The logical units of the board were grouped in 3 different ways: by function, by communication bus and by I/O expander reach. Grouping is described according to Figure 7.

First of all, units are grouped by functionality. MCU with its dedicated bus switches is placed in the center (30). Debugging components were brought to the right side of the board (19-22). Analog sensors with ADCs were placed near the bottom of the board (10-18). Digital sensors were placed on the left side of the board (1-9). MCU supplementary ICs were placed at the top of the board (23-27). I/O expanders (28-29) are placed close to the MCU.

Secondly, devices were grouped according to the communication buses used by the devices. Seven devices communicate through SPI4 (1-3, 25-28). Only four ICs (4-7) communicate through SPI2, but SPI2 is also used to communicate to any additional sensors that can be connected to the board. Similarly to SPI4, SPI3 is used by seven ICs (10-15, 29) to communicate with the MCU.

Thirdly ICs were grouped by separating the influence of two I/O expanders. I/O expanders are only used for mostly constant signals like power and bus switch enable or analog sensors selftest or mode select signals. First I/O expander controls seven ICs (12-18), which include analog sensors and their signals. Second I/O expander controls devices 13 ICs (1-11, 26-27).

Some very sensitive ICs like ADCs and magnetometer require explicit layout considerations. Magnetometer is a sensitive IC. It is recommended to avoid placing traces with currents higher than 10 mA closer than at a few millimeters distance, or it will affect magnetic field measurements [43]. It is recommended not to place digital signal traces under the ADCs, thus avoid digital signal interfering with the measurements. Actually all analog and digital electronics should be separated, but it was impossible to separate the voltage and temperature measurement traces from digital electronics entirely. Therefore it was attempted to minimize the digital signal influence by bringing the analog signals to the side of the board, maximizing the distance between analog and digital signals and occasionally placing traces on the inner layer.

Communication interfaces are mostly placed at sides of the board to allow easy access and reduce interference of additional wires.

The prototype board is planned to be ordered from Brandner PCB manufacturer company. The design has to take into consideration manufacturer capabilities and recommendations. Pushing to the manufacturer limits will increase the price of board manufacturing, which should be also avoided. For example Brandner allows 0.1 mm drilled holes, but the prototype uses a minimum hole diameter of 0.3 mm. The minimal allowed gap between traces is 0.05 mm, but the prototype board

layout has been done with a minimum of 0.14 mm gap. This increasing the possible error margin for the manufacturer. [71]

4.4.3 Result

A 110 mm × 115 mm AOCS prototype board has been designed. The design satisfies all of the prototype requirement stated in this thesis.

- The double switch concept and its implementation allows turning off all sensor and ADCs independently.
- Redundancy for each type of sensors is provided by the prototype board design.
- The board allows testing of a range of different sensors by exploiting the redundancy requirement.
- Interfaces for communication testing and evaluation of external devices are provided.
- Interrupts are used for measurement completion indication to simplify the firmware development.
- Each sensor power supply voltage and temperature are measured by an on-board ADC.
- Prototype is able to work from a battery, which simplifies hardware testing.
- Board design provides debugging facilities for hardware and software.

Explicit hardware requirements are fulfilled. Summary of most important integrated circuits used in the design:

- Six gyroscopic sensors, two analog and four digital;
- Three accelerometers, one analog and two digital;
- Three magnetometers, all digital;
- Two 24-bit low noise analog-to-digital converters for analog sensors;
- Four 12-bit analog-to-digital converters for Sun sensor, temperature and power supply measurements;
- A MCU with FPU, sufficient peripherals and low power consumption;
- 20 load switches for power management;
- 4-bit, 10-bit and 24-bit bus switches for power management;
- USB interface for different communication buses;
- LDOs for standalone usage.

4.5 AOCS Prototype Analysis and Firmware Development

This section shortly describes further prototype development plan as well as current developments in AOCS firmware. The result of this thesis is a board design, which has to be assembled, tested and analyzed for flaws before it can be used for firmware development.

The prototype is planned to be assembled by the author after submission of this thesis. Tartu Observatory will provide all required tools for the assembly and testing. Even though great effort was put into the design to avoid schematic and board layout errors, it cannot be assumed that the board is flawless. Therefore all flaws found in the board design will be reported and analyzed. This analysis will be used in further AOCS main board development.

After the platform is assembled and tested, it can be used for firmware development. AOCS algorithms require very strict scheduling, which could be achieved only by a real-time operating system. Currently two possibilities are considered.

First solution would be to reuse the ESTCube-1 Command and Data Control Systems freeRTOS operation system. ESTCube team is more familiar it and some drivers would be easily rewritten for the new platform. At the same time there will be a different operating system for the On-Board Computer, which will complicate the ESTCube-2 firmware as a whole.

The second solution would be to also migrate to a Linux like operating system of On-Board Computer. Similarity of the operating systems will simplify future development, but initial firmware development will be staggered because of the lack of experience.

Selection of the operating system will be performed after initial tests on AOCS prototype will be performed. After the selection, drivers for all hardware components must be written. That includes information gathering and actuator control drivers. Power management drivers should be also thoroughly tested. Consequently AOCS algorithms can be developed and tested as well as it is possible on Earth.

ESTCube-2 mission is to test the satellite technologies in orbit for ESTCube-3 mission, hence the next step will be to test the AOCS algorithms in low Earth orbit.

5 Summary

ESTCube-1, the first Estonian student satellite, has been in orbit for more than a year. It already has fulfilled most of its objectives. The main scientific experiment is yet to be performed, but ESTCube team gained enormous amount of space technology development experience. Therefore it should come as no surprise that the team is already planning the future space missions, which depend on having a high accuracy Attitude and Orbit Control System (AOCS).

First the thesis introduces future ESTCube missions and their objectives. Then requirements and structure of ESTCube-2 AOCS are described, followed by an analysis of the previous attitude and orbit determination and control hardware solutions from other nanosatellites.

The prototype board of ESTCube-2 AOCS has been designed as a result of this work. Design included new hardware selection, introducing a new double bus switch concept for power management, creating the electronics schematics and designing the layout of the board. The design fulfills all of the AOCS prototype board requirements.

Although fulfillment of main AOCS requirements cannot be confirmed before an actual flight, the AOCS prototype should provide desired accuracy according to previous attitude and orbit control solutions review. Naturally the hardware requires development of AOCS algorithms, which would allow to achieve such accuracy.

The AOCS prototype main board with its hardware is yet to be assembled and tested, so the work is to be continued after this thesis is submitted. After hardware assembly and testing is done, AOCS firmware is to be developed on the designed platform.

6 Acknowledgements

I would like to thank my supervisors Andris Slavinskis and Viljo Allik for their support and sharing their knowledge. They guided me in topics of satellite building and electronics design. I have learned a lot from them.

I would like to express my gratitude to all ESTCube team members as well as instructors, who shared their knowledge with me. Many thanks to Tõnis Eenmäe, Jaan Viru and Erik Ilbis in that respect. Special thanks to Indrek Sünter, Kaspars Laizans and Jaanus Kalde for helping me design and reviewing the prototype board. Thanks to Karoli Kahn for managing the ETSCube-2 project.

I would like to thank Silver Lätt and Mart Noorma for managing the whole student satellite program.

Finally I am grateful to my family who supported me morally throughout the project.

ESTCube-2 asendi ja orbiidi juhtimissüsteemi prototüüpi disain

Georgi Olentšenko

Kokkuvõte

Esimene Eesti satelliit ESTCube-1 viidi edukalt maalähedasele orbiidile 2013. aasta maikuu ning aasta vältel on satelliit täitnud peaaegu kõik oma eesmärgid välja arvatud päikesepurje eksperiment [7]. Eksperimendi jooksul pannakse satelliit pöörlema kiirusega 1 pööre sekundis, keritakse 10 m pikkune mikrojuhe välja ning laetakse see kõrge potentsiaalini. Teoreetiliselt peaks laetud mikrojuhtme ja Maa ionosfäärilise plasma vastasmõju toimel satelliidi pöörlemiskiirus kahanema [14]. Kuigi missioon pole veel lõppenud, plaanitakse juba Eesti Tudengisatelliidi programmi raames järgmisi missioone [11].

Üks ESTCube-2 ja ESTCube-3 missioonide eesmärkidest on jätkata päikesepurje testimist, kasutades 1 km pikkusega mikrojuhet. Teiseks eesmärgiks on demonstreerida *NanoSpace Cold Gas thruster*'i kasutamist asendi ja orbiidi juhtimissüsteemi mootorina [12]. Mõlemat meetodit saab potentsiaalselt kasutada kosmoses reisimiseks [13].

Magistritöö jooksul arendati uut satelliidi asendi ja orbiidi juhtimissüsteemi, mis on hädavajalik missioonide teaduslike eesmärkide täitmiseks. Magistritöö eesmärkideks oli:

- tuua välja nõuded ESTCube-2 asendi ja orbiidi juhtimissüsteemi jaoks;
- kirjeldada süsteemi struktuuri;
- tuua välja nõuded satelliidi asendi ja orbiidi juhtimissüsteemi prototüüplaadi jaoks;
- valida riistavara prototüüplaadi jaoks;
- arendada satelliidi asendi ja orbiidi juhtimissüsteemi esimene prototüüplaat.

Prototüüplaadi konstruktsioon põhineb ESTCube-1 asendi juhtimissüsteemil ja ESTCube meeskonna kogemustel. Tulevalt uute missioonide poolt esitatavatest nõuetest on vajalik ka täiendava riistvara lisamine ning süsteemi suurema jõudluse garanteerimine. On analüüsitud teiste nanosatelliitide lahendused. Töö jooksul oli valitud uued elektroonikakomponendid ja kasutatud uued konstruktsioonilahendusi, mis välistavad ESTCube-1 konstruktsioonis leitud puudusi.

Tulemuseks on saadud kõikidele nõudmistele vastav prototüüplaadi konstruktsioon. Prototüüplaat võimaldab välja lülitada kõik andurid ühe kaupa, võimaldab korraga läbi testida valikut sobivaid andureid ja võimaldab efektiivselt testida vajalikke riistvara- ja tarkvarakomponente.

Töö tulemuseks on prototüüplaadi konstruktsioon, mida on valmis kokkumonteerimiseks ja testimiseks. Seega peale magistritöö esitamist kavatseb autor tööd jätkata ning arendada tarkvara konstrueeritud platvormi jaoks.

References

- [1] “CubeSat Design Specification,” The CubeSat Program, California Polytechnic State University, January 8, 2009.
- [2] Artur Scholz, Felix König, Steve Fröhlich, Johannes Piepenbrock, “Flight Results of the COMPASS-1 Mission,” March 8, 2009, <http://www.raumfahrt.fh-aachen.de/compass-1/download/COMPASS-1%20Flight%20Results.pdf> (accessed May 23, 2014).
- [3] “STRaND-1: Smartphone nanosatellite,” <http://www.sstl.co.uk/Missions/STRaND-1--Launched-2013/STRaND-1/STRaND-1--Smartphone-nanosatellite> (accessed April 28, 2014).
- [4] A. Kestilä, T. Tikka, P. Peitso, J. Rantanen, A. Näsilä, K. Nordling, H. Saari, R. Vainio, P. Janhunen, J. Praks, M. Hallikainen, “Aalto-1 nanosatellite – technical description and mission objectives,” *Geoscientific Instrumentation, Methods and Data Systems*, 2, 121–130, 2013.
- [5] “SwissCube,” <https://directory.eoportal.org/web/eoportal/satellite-missions/s/swisscube> (accessed April 28, 2014).
- [6] “Radio Aurora Explorer,” <http://rax.engin.umich.edu/> (accessed April 28, 2014).
- [7] Silver Lätt, Andris Slavinskis, Erik Ilbis, Urmas Kvell, Kaupo Voormansik, Erik Kulu, Mihkel Pajusalu, Henri Kuuste, Indrek Sünter, Tõnis Eenmäe, Kaspars Laizans, Karlis Zalite, Riho Vendt, Johannes Piepenbrock, Ilmar Ansko, Ahto Leitu, Andres Vahter, Ants Agu, Elo Eilonen, Endel Soolo, Hendrik Ehrpais, Henri Lillmaa, Ivar Mahhonin, Jaak Mõttus, Jaan Viru, Jaanus Kalde, Jana Šubitidze, Jānis Mucenieks, Jānis Šate, Johan Kütt, Juris Poļevskis, Jürgen Laks, Kadi Kivistik, Kadri-Liis Kusmin, Kalle-Gustav Kruus, Karl Tarbe, Katrin Tuude, Katrīna Kalniņa, Laur Joost, Marko Lõoke, Markus Järve, Mart Vellak, Martin Neerot, Martin Valgur, Martynas Pelakauskas, Matis Averin, Mats Mikkor, Mihkel Veske, Ott Scheler, Paul Liias, Priit Laes, Ramon Rantsus, Reimo Soosaar, Risto Reinumägi, Robert Valner, Siim Kurvits, Sven-Erik Mändmaa, Taavi Ilves, Tanel Peet, Tavo Ani, Teet Tilk, Timothy Henry Charles Tamm, Tobias Scheffler, Toomas Vahter, Tõnis Uiboupin, Veigo Evard, Andreas Sisask, Lauri Kimmel, Olaf Krömer, Roland Rosta, Pekka Janhunen, Jouni Envall, Petri Toivanen, Timo Rauhala, Henri Seppänen, Jukka Ukkonen, Edward Haeggström, Risto Kurppa, Taneli Kalvas, Olli Tarvainen, Janne Kauppinen, Antti Nuottajärvi, Hannu Koivisto, Sergiy Kiprich, Alexander Obraztsov, Viljo Allik, Anu Reinart, Mart Noorma, “ESTCube-1 nanosatellite for electric solar wind sail in-orbit technology

- demonstration,” *Proceedings of the Estonian Academy of Sciences*, 2014, 63, 2S, 200–209.
- [8] Pekka Janhunen, “Electric sail for spacecraft propulsion,” *AIAA Journal of Propulsion and Power*, 20 (4), 763–764, August 2004.
- [9] Pekka Janhunen, Arto Sandroos, “Simulation study of solar wind push on a charged wire: basis of solar wind electric sail propulsion,” *Annales Geophysicae*, 25, 755–767, 2007.
- [10] P. Janhunen, P. K. Toivanen, J. Polkko, S. Merikallio, P. Salminen, E. Haeggström, H. Seppänen, R. Kurppa, J. Ukkonen, S. Kiprich, G. Thornell, H. Kratz, L. Richter, O. Krömer, R. Rosta, M. Noorma, J. Envall, S. Lätt, G. Mengali, A. A. Quarta, and H. Koivisto, "Invited Article: Electric solar wind sail: Toward test missions," *Review of Scientific Instruments*, no. 81, 2010.
- [11] Mart Noorma, Erik Kulu, Andris Slavinskis, Mihkel Pajusalu, Urmas Kvell, Silver Lätt, “Estonian Student Satellite Program,” *64th International Astronautical Congress*, Beijing, China, IAC-13.E1.3.5, 2013.
- [12] Urmas Kvell, Marit Puusepp, Franz Kaminski, Jaan-Eerik Past, Kristoffer Palmer, Tor-Arne Grönland, Mart Noorma, “Nanosatellite orbit control using MEMS cold gas thrusters”, *Proceedings of the Estonian Academy of Sciences*, 2014, 63, 2S, 279–285. NanoSpace
- [13] Pekka Janhunen, Sini Merikallio, Petri Toivanen, Jouni Envall, Jouni Polkko, “Possibilities opened by electric solar wind sail technology,” *63rd International Astronautical Congress*, Naples, Italy, IAC-12-D4.1.4, 2012.
- [14] Jouni Envall, Pekka Janhunen, Petri Toivanen, Mihkel Pajusalu, Erik Ilbis, Jaanus Kalde, Matis Averin, Henri Kuuste, Kaspars Laizans, Viljo Allik, Timo Rauhala, Henri Seppänen, Sergiy Kiprich, Jukka Ukkonen, Edward Haeggström, Taneli Kalvas, Olli Tarvainen, Janne Kauppinen, Antti Nuottajärvi, Hannu Koivisto, “E-Sail test payload of ESTCube-1 nanosatellite,” *Proceedings of the Estonian Academy of Sciences*, 2014, 63, 2S, 210–221.
- [15] Pekka Janhunen, Petri Toivanen, Jouni Envall, Sini Merikallio, Giuditta Montesanti, Jose Gonzalez del Amo, Urmas Kvell, Mart Noorma, Silver Lätt, “Overview of electric solar wind sail applications,” *Proceedings of the Estonian Academy of Sciences*, 2014, 63, 2S, 267–278.
- [16] Henri Seppänen, Timo Rauhala, Sergiy Kiprich, Jukka Ukkonen, Martin Simonsson, Risto Kurppa, Pekka Janhunen, Edward Hæggström, “One kilometer (1 km) electric solar wind sail tether produced automatically,” *Review of Scientific Instruments*, 84, 095102, 2013.
- [17] Pekka Janhunen, “Increased electric sail thrust through removal of trapped shielding

- electrons by orbit chaotisation due to spacecraft body,” *Annales Geophysicae*, 27, 3089-3100, 2009.
- [18] CubeSat MEMS Propulsion Module, [http://www.sscspace.com/\\$2/file/cubesat-mems-propulsion-module.pdf](http://www.sscspace.com/$2/file/cubesat-mems-propulsion-module.pdf) (accessed May 16, 2014).
- [19] Andris Slavinskis, Erik Kulu, Jaan Viru, Robert Valner, Hendrik Ehrpais, Tõnis Uiboupin, Markus Järve, Endel Soolo, Jouni Envall, Tobias Scheffler, Indrek Sünter, Henri Kuuste, Urmas Kvell, Jaanus Kalde, Kaspars Laizans, Erik Ilbis, Tõnis Eenmäe, Riho Verdt, Kaupo Voormansik, Ilmar Ansko, Viljo Allik, Silver Lätt, Mart Noorma, “Attitude determination and control for centrifugal tether deployment on the ESTCube-1 nanosatellite,” *Proceedings of the Estonian Academy of Sciences*, 2014, 63, 2S, 242–249.
- [20] Andris Slavinskis, Urmas Kvell, Erik Kulu, Indrek Sünter, Henri Kuuste, Silver Lätt, Kaupo Voormansik, Mart Noorma, “High spin rate magnetic controller for nanosatellites,” *Acta Astronautica*, 2014, 95, 218-226.
- [21] Kaspars Laizans, Indrek Sünter, Karlis Zalite, Henri Kuuste, Martin Valgur, Karl Tarbe, Viljo Allik, Georgi Olentšenko, Priit Laes, Silver Lätt, Mart Noorma, “Design of the fault tolerant command and data handling subsystem for ESTCube-1,” *Proceedings of the Estonian Academy of Sciences*, 2014, 63, 2S, 222–231.
- [22] Stefano Rossi, Anton Ivanov, Muriel Richard, Volker Gass, Armin Roesch, “Four years (almost) of SwissCube operations” CubeSat Summer Workshop 2013, August 10-11, 2013, Utah State University, Logan, Utah.
- [23] “CanX-4&5 (Canadian Advanced Nanospace eXperiment-4&5),” <https://directory.eoportal.org/web/eoportal/satellite-missions/c-missions/canx-4-5> (accessed May 17, 2014).
- [24] “CubeSat ADCS,” Clyde Space, <http://www.clyde-space.com/documents/2438> (accessed May 17, 2014).
- [25] “UKube-1 (United Kingdom Universal Bus Experiment 1),” <https://directory.eoportal.org/web/eoportal/satellite-missions/u/ukube-1> (accessed May 17, 2014).
- [26] “Future FUNcube missions – 2014 launch dates,” <http://amsat-uk.org/2014/05/07/future-funcube-missions-2014-launch-dates/> (accessed May 17, 2014).
- [27] Igal Kronhaus, Klaus Schilling, Satish Jayakumar, Alexander Kramer, “Design of the UWE-4 Picosatellite Orbit Control System using Vacuum-Arc-Thrusters,” *33rd International*

- Electric Propulsion Conference*, The George Washington University, Washington, D.C., USA, October 6–10, 2013.
- [28] Philip Bangert, Stephan Busch, Klaus Scilling, “Performance characteristics of the UWE-3 miniature attitude determination and control system,” *IAA Conference on Dynamics and Control of Space Systems*, IAA-AAS-DyCoSS2-14-05-07, 2007.
- [29] Osama Khurshid, Tuomas Tikka, Jaan Praks, Martti Hallikainen, “Accommodating the plasma brake experiment on-board the Aalto-1 satellite,” *Proceedings of the Estonian Academy of Sciences*, 2014, 63, 2S, 258–266.
- [30] “iADCS-100 Intelligent Attitude Control for CubeSats,” Berlin Space Technologies, http://www.berlin-space-tech.com/fileadmin/media/BST_iACDS-100_Flyer.pdf (accessed May 16, 2014).
- [31] LPC3180, 16/32-bit ARM MCU, data sheet, NXP semiconductors, Rev. 2, February 2007.
- [32] “STM32F4 Series comparison,” STMicroelectronics, <http://www.st.com/web/en/catalog/mmc/FM141/SC1169/SS1577> (accessed May 18, 2014).
- [33] FM25V20, 2-Mbit Serial (SPI) FRAM, Cypress, Rev. D, January 2014.
- [34] DS3234, SPI Bus RTC, Maxim Integrated, Rev. 3, July 2011.
- [35] ITG-3200, 3-axis digital gyroscopic sensor, production specification, InvenSense, Inc., Rev. 1.7, 2007.
- [36] MAX21000, 3-axis digital gyroscopic sensor, data sheet, Maxim Integrated, Rev. 1, February 2013.
- [37] BMG160, 3-axis digital gyroscopic sensor, data sheet, Bosch Sensortec, Rev. 1.1, November 2013.
- [38] MPU-6000 and MPU-6050 motion sensors, product specification, InvenSense Inc., Rev. 3.4, August 2013.
- [39] L3GD20H, 3-axis digital gyroscopic sensor, data sheet, STMicroelectronics, Rev. 2, March 2013.
- [40] LPY403AL, 2-axis analog gyroscopic sensor, data sheet, STMicroelectronics, Rev. 1, October 2009.
- [41] LPR403AL, 2-axis analog gyroscopic sensor, data sheet, STMicroelectronics, Rev. 1, October 2009.
- [42] HMC5883L, 3-axis digital magnetometer, data sheet, Honeywell, Rev E, February 2013.

- [43] LIS3MDL, 3-axis digital magnetometer, data sheet, STMicroelectronics, Rev 2, April 2013.
- [44] MAG3110, 3-axis digital magnetometer, data sheet, Freescale Semiconductor, Inc., Rev. 9.2, February 2013.
- [45] LSM303D, digital 3-axis magnetometer and 3-axis accelerometer, data sheet, STMicroelectronics, Rev 2, November 2013.
- [46] FXOS8700CQ, digital 3-axis magnetometer and 3-axis accelerometer, data sheet, Freescale Semiconductor, Inc., Rev. 3.0, July 2013.
- [47] KXRB5-2050, 3-axis analog accelerometer, data sheet, Kionix, Inc., Rev. 1, October 2009.
- [48] FXLC95000L, motion-sensing platform, data sheet, Freescale Semiconductor, Inc., Rev. 1.2, August 2013.
- [49] 393B04 seismic accelerometer, specification, PCB Piezotronics, Inc., <http://www.pcb.com/products.aspx?m=393B04> (accessed May 23, 2014).
- [50] SF1600S.A – SF1600SN.A, seismic accelerometer, data sheet, Colybris, November 2011.
- [51] MAX1226/MAX1228/MAX1230, 12-bit ADC, data sheet, Maxim Integrated, Rev. 5, December 2010.
- [52] MAX11626-MAX1633, 12-bit ADC, data sheet, Maxim integrated products Inc., Rev. 4, October 2011
- [53] AD7490, 12-bit ADC, data sheet, Analog Devices, Inc., Revision D, December 2012.
- [54] AD7708/AD7718, 24-bit ADC, data sheet, Analog Devices, Inc., Rev. 0, August 2001
- [55] AD7173-8, 24-bit ADC, data sheet, Analog Devices, Inc., Rev. A, April 2014
- [56] KTY82, resistive temperature sensor, data sheet, NXP semiconductors, Rev. 4, January 2008
- [57] LMT86/LMT86-Q1, analog temperature sensor, data sheet, Texas Instruments, June 2013.
- [58] ADR3412/ADR3420/ADR3425/ADR3430/ADR3433/ADR3440/ADR3450, voltage reference, data sheet, Rev. B, June 2010.
- [59] TPS22941/TPS22942/TPS22943/TPS22944/TPS22945, load switch, data sheet, Texas Instruments, November 2009.
- [60] SN74CBTLV16211, 24-bit bus switch, data sheet, Texas Instruments, October 2003.
- [61] SN74CBTLV3384, 10-bit bus switch, data sheet, Texas Instruments, Rev. G, July 2004.
- [62] SN74CBTLV3126, 4-bit bus switch, data sheet, Texas Instruments, Rev. I, October 2003.
- [63] MCP23017/MCP23S17, 16-bit I/O Expander, data sheet, Microchip Technology, Rev. B, February 2007.

- [64] LM1117-N/LM1117I, 800 mA LDO Regulator, Texas Instruments, March 2013.
- [65] LP2992, 250 mA LDO Regulator, data sheet, Texas Instruments, March 2013.
- [66] LMP8645/LMP8645HV, current sense amplifier, Texas Instruments, March 2013.
- [67] FT200X, USB I2C SLAVE IC, data sheet, Future Technology Devices International Ltd., Rev. 1.3, 2013.
- [68] FT220X, USB SPI SLAVE IC, data sheet, Future Technology Devices International Ltd., Rev. 1.3, 2013.
- [69] FT230X, USB TO BASIC UART, data sheet, Future Technology Devices International Ltd., Rev. 1.3, 2013.
- [70] "Printed-Circuit-Board Layout for Improved Electromagnetic Compatibility," October, Texas Instruments, October 1996.
- [71] "Production Capabilities, Brandner PCB, " <https://www.brandner.ee/eng/74/83> (Accessed May 19, 2014).

Appendices

Appendix A – Prototype Board Schematic

Sensors group

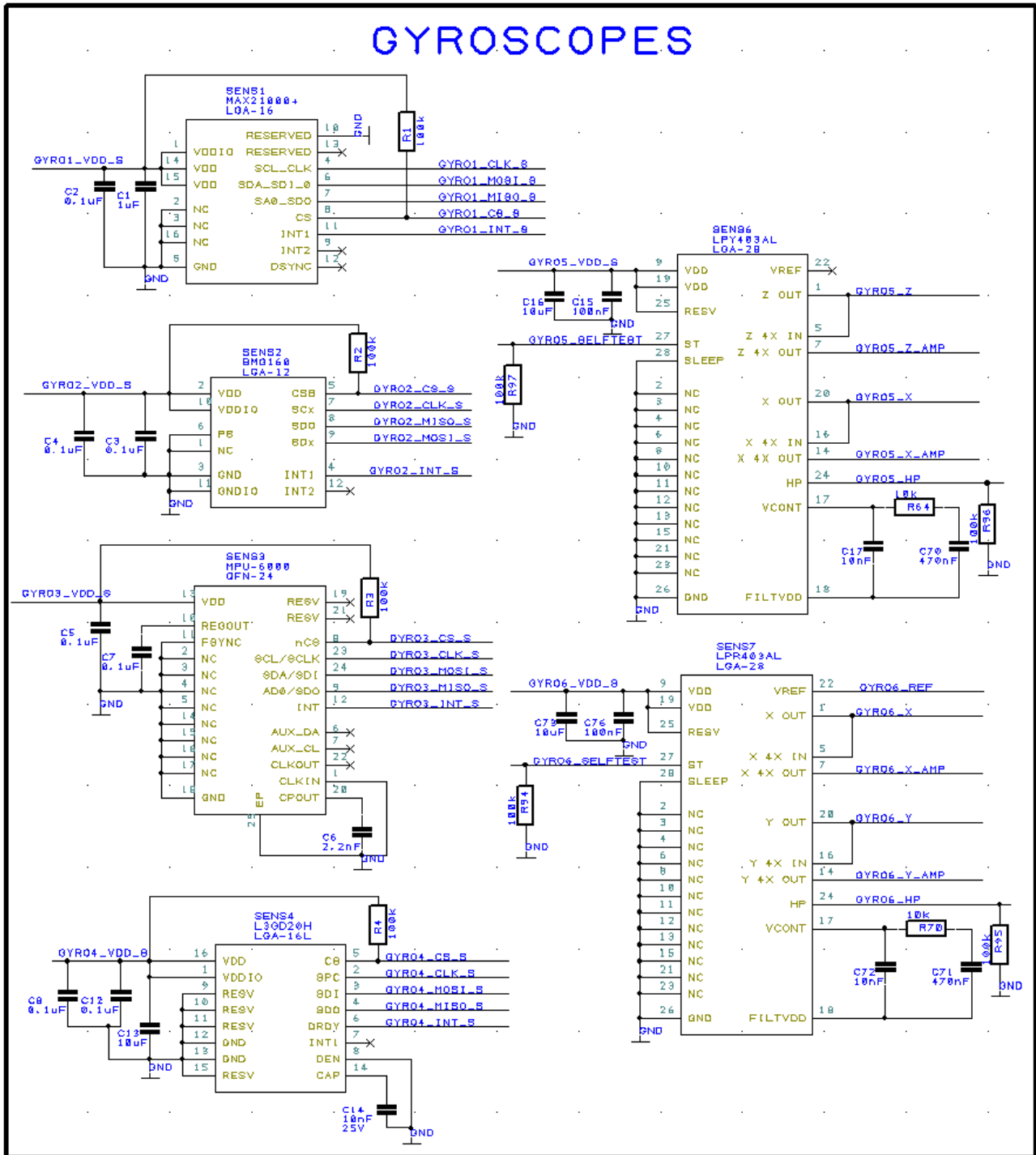


Figure 8: MAX21000, BMG160, MPU-6000, L3GD20H, LPY403AL and LPR403AL gyroscopes.

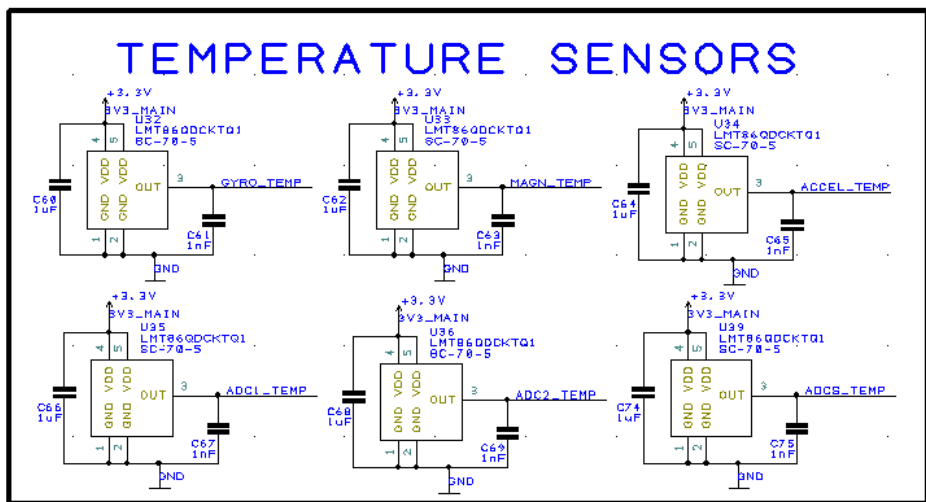
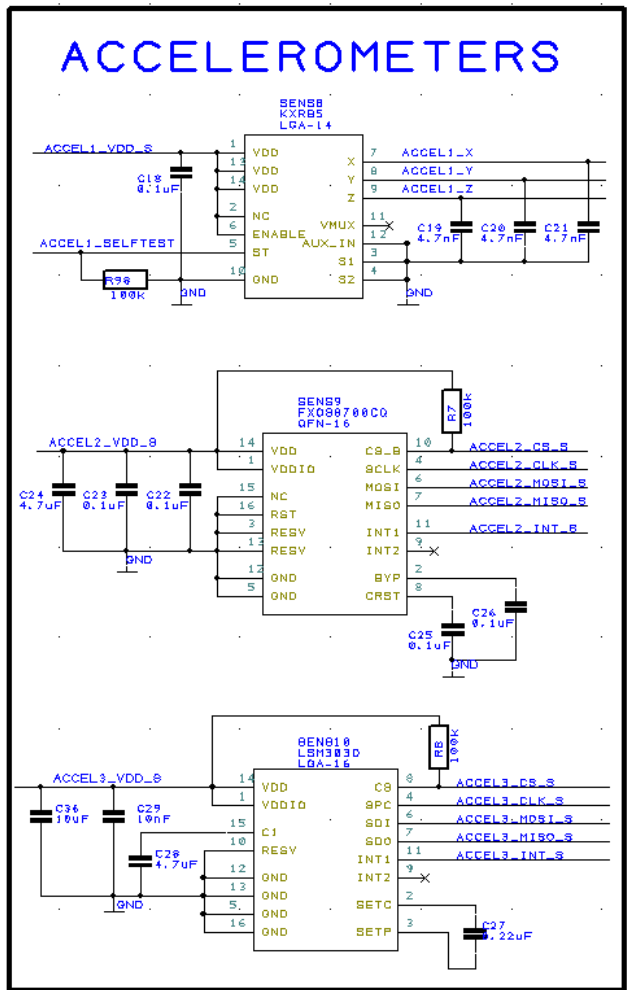
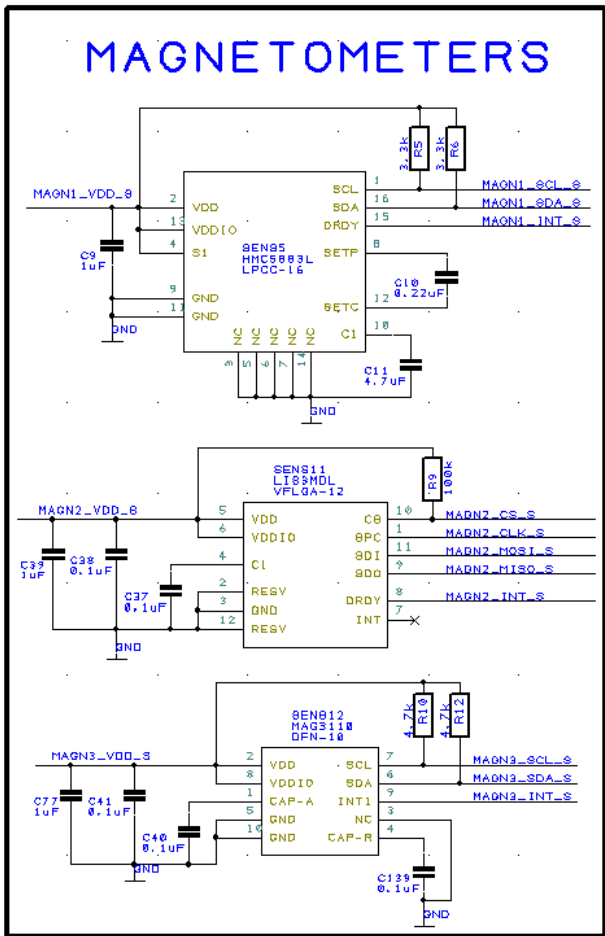


Figure 9: Upper left: HMC5883L, LIS3MDL and MAG3110 magnetometers. Upper right: KXR85,FXC8700CQ and LSM303D accelerometers. Bottom: six LMT86 temperature sensors.

ADCs group

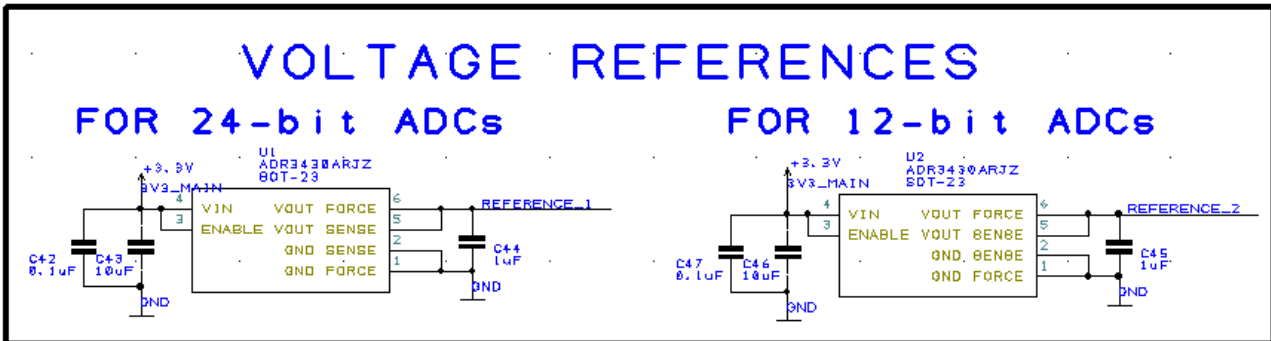
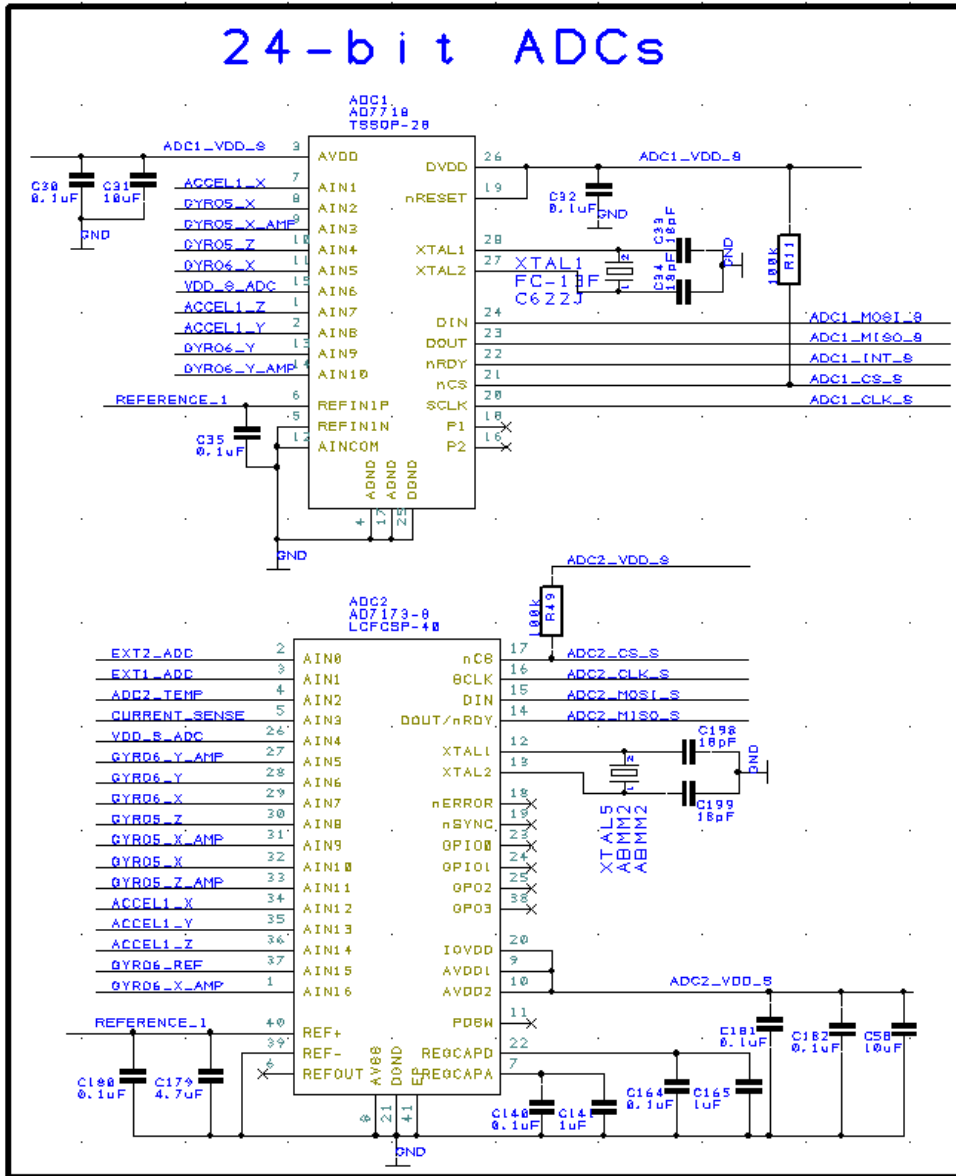


Figure 10: Top: AD7710 and AD7173 24-bit analog-to-digital converters. Bottom: two voltage references.

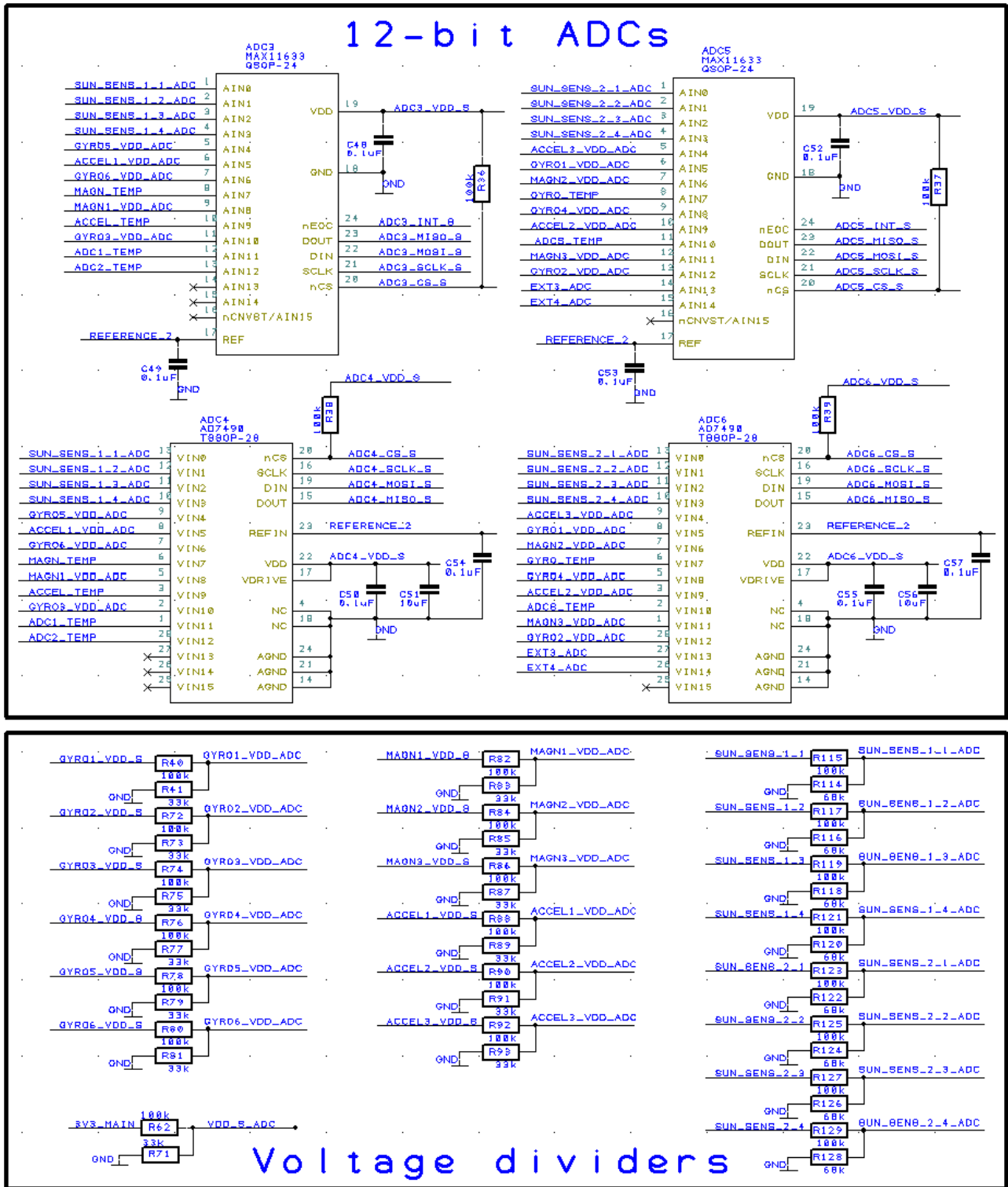


Figure 11: Top: two MAX11633 and two AD7490 12-bit analog-to-digital converters. Bottom: voltage dividers for power supply and Sun sensors measurements.

Power management group

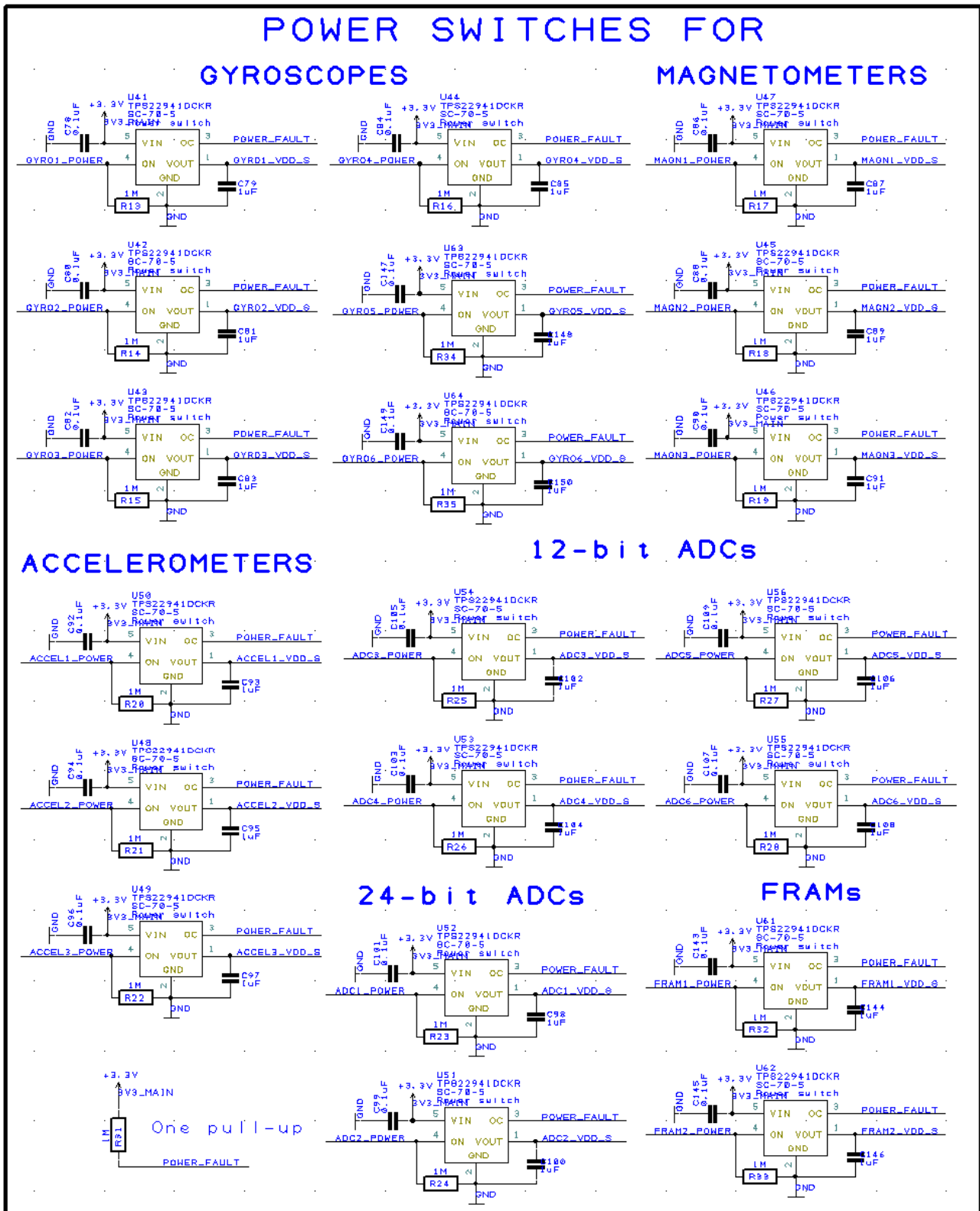


Figure 12: There are 20 power switched for all sensors, ADCs and FRAMs.

BUS SWITCHES FOR ADCs

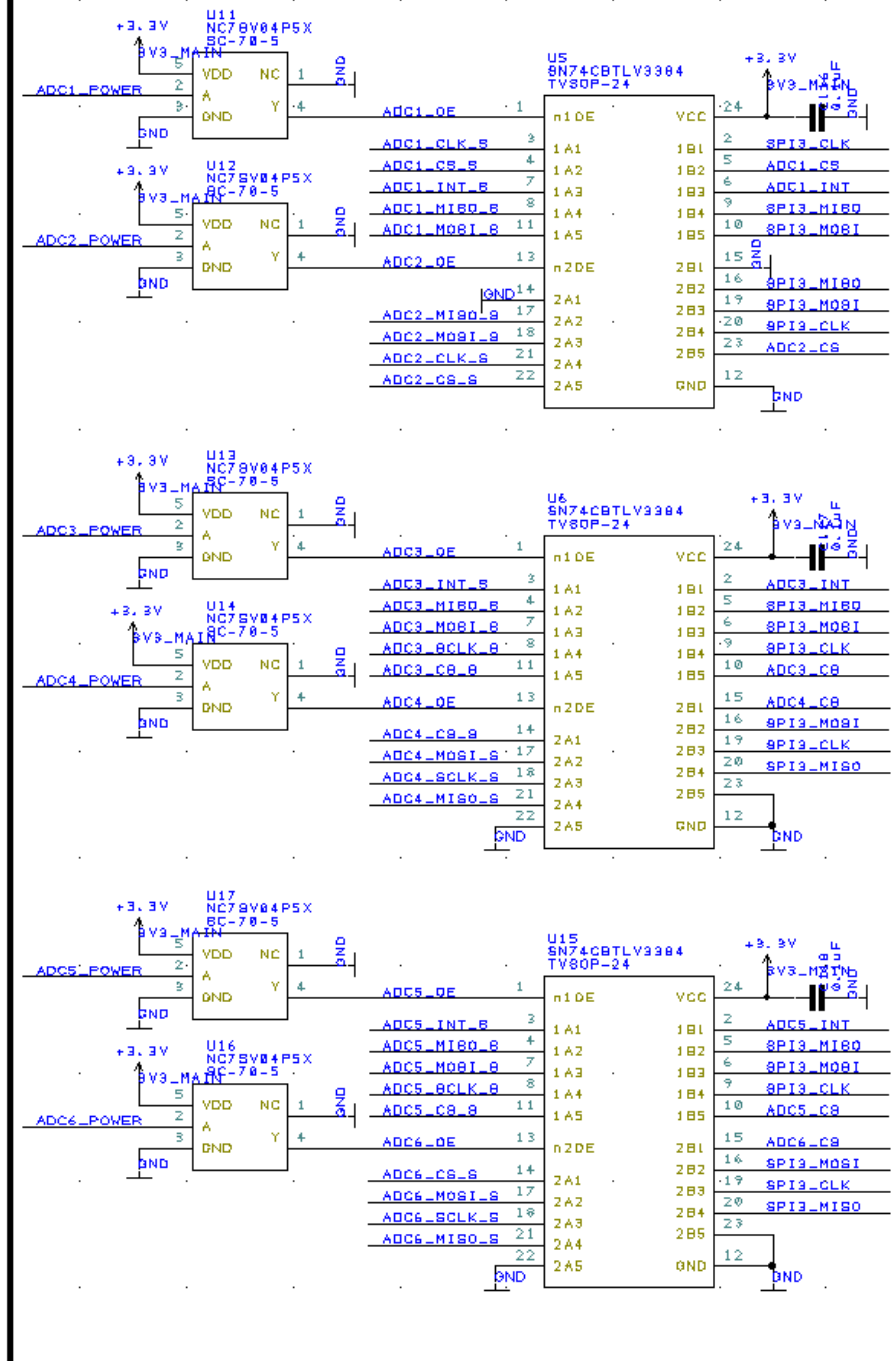
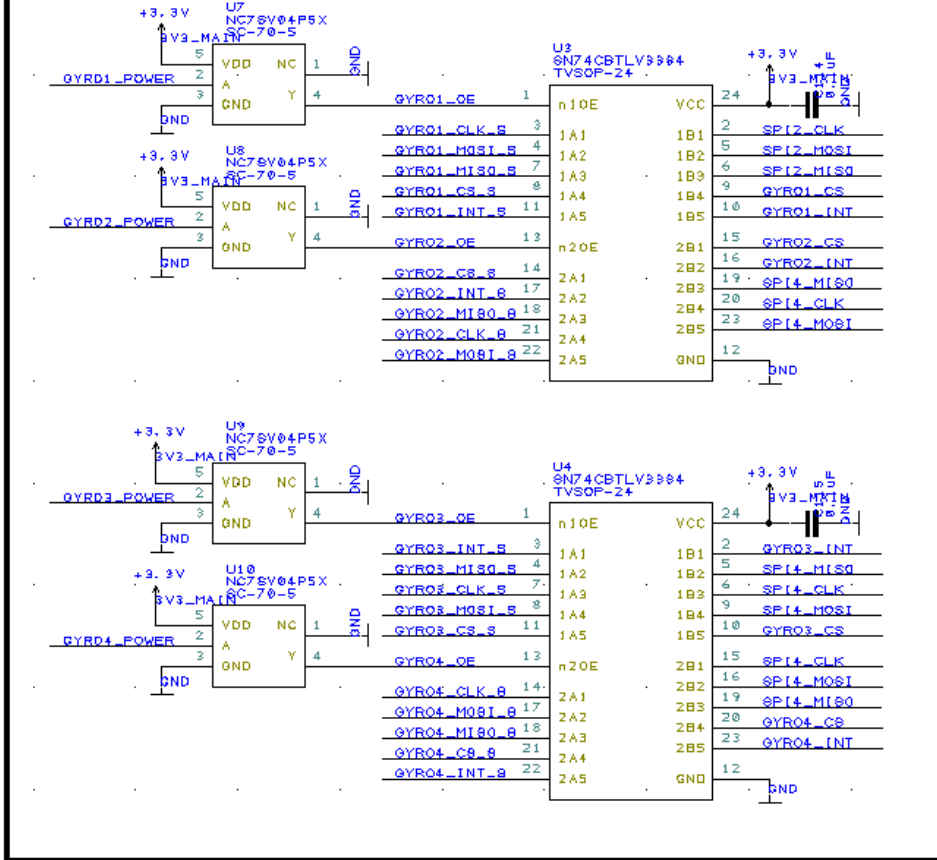


Figure 13: Three 10-bit bus switches for ADCs.

BUS SWITCHES FOR DIGITAL GYROSCOPES



BUS SWITCH FOR DIGITAL ACCELEROMETERS

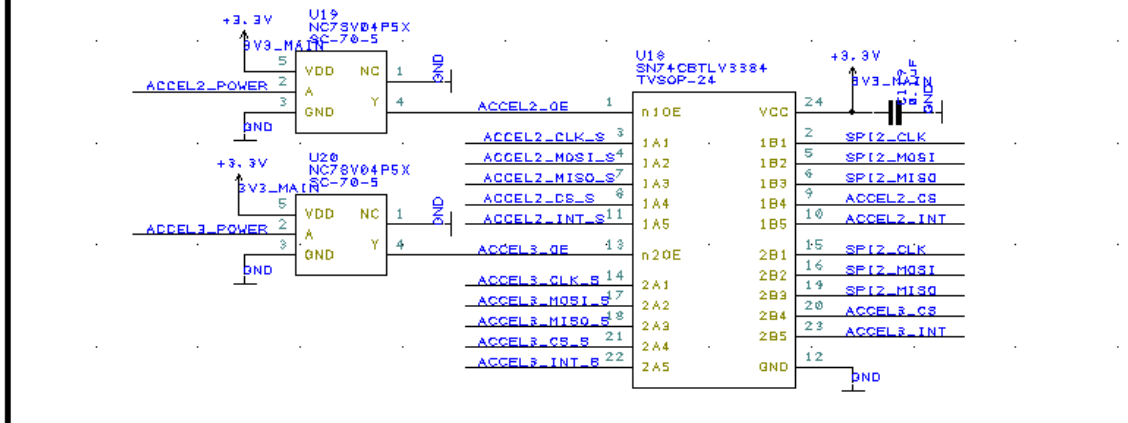


Figure 14: Top: two 10-bit bus switches for digital gyroscopes. Bottom: one 10-bit bus switch for digital accelerometers.

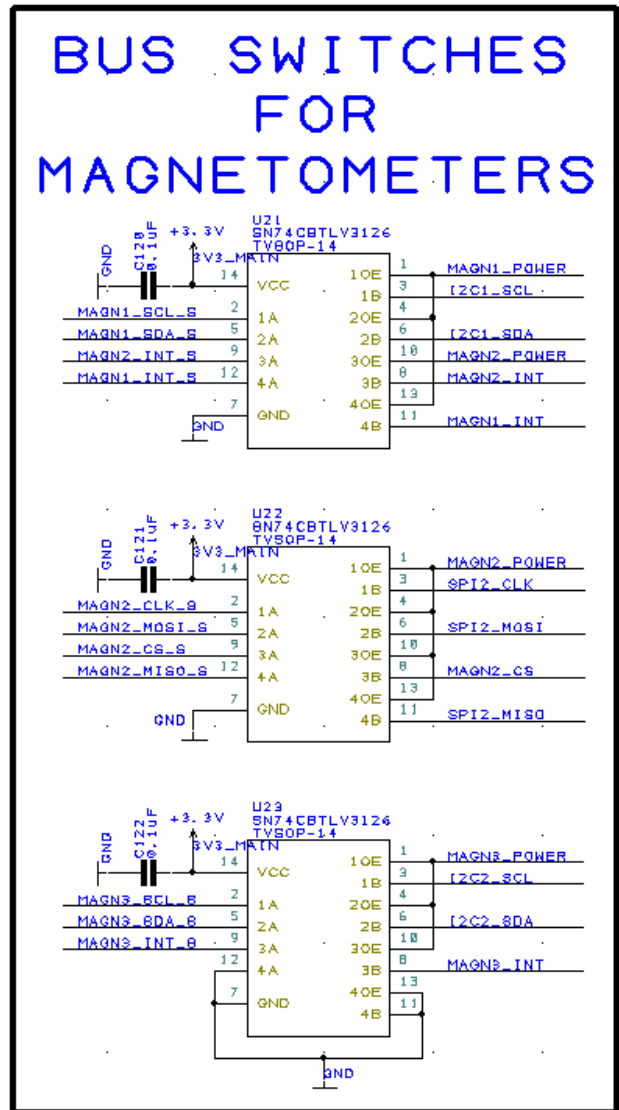
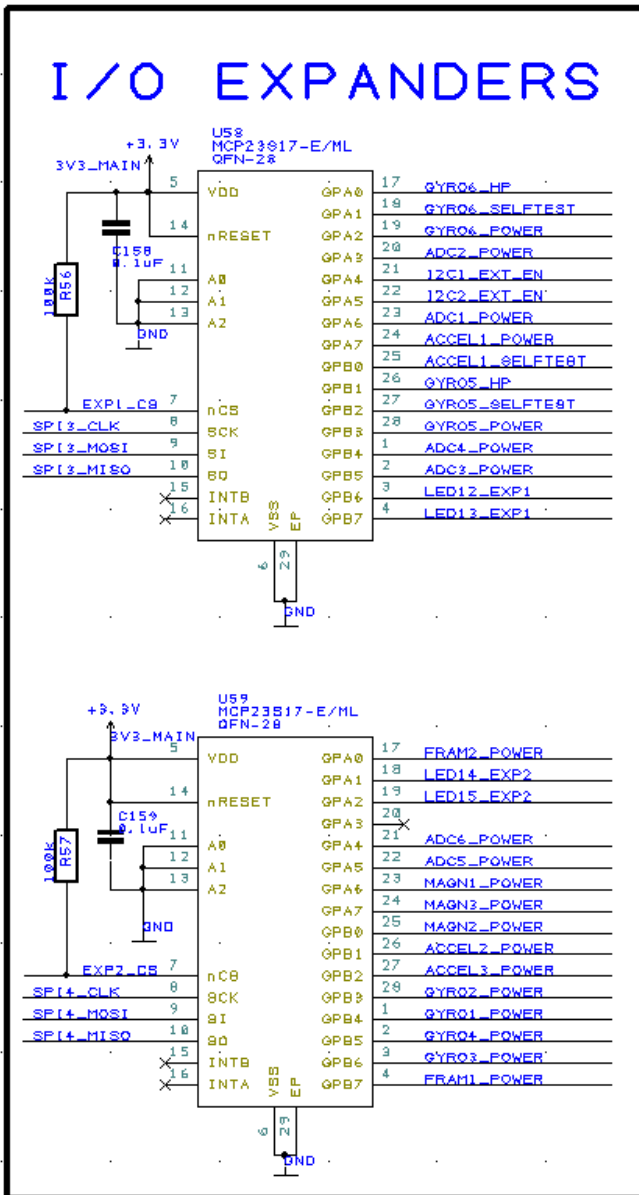


Figure 15: Left: two I/O expanders for power management. Right: three 4-bit bus switches for digital magnetometers.

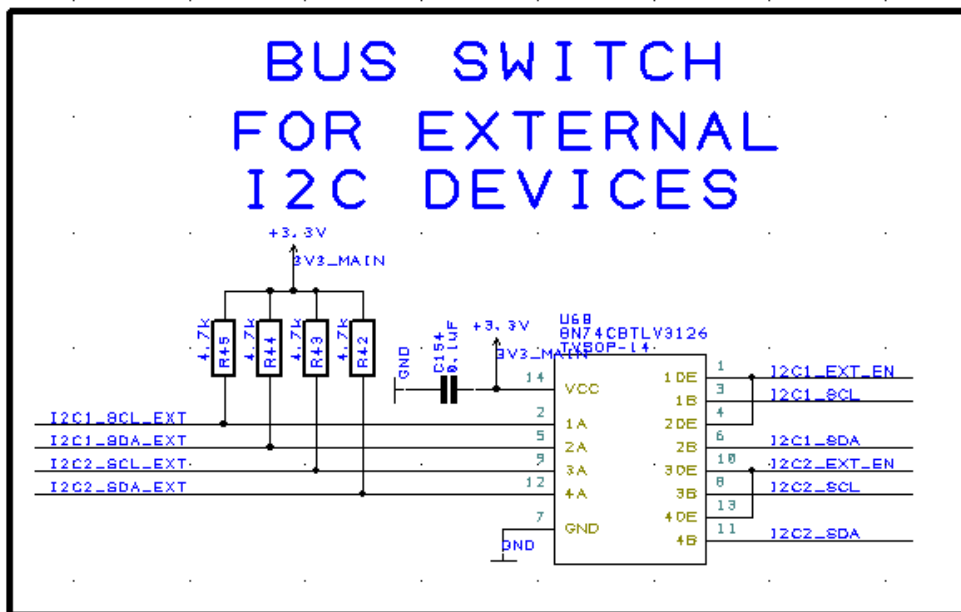
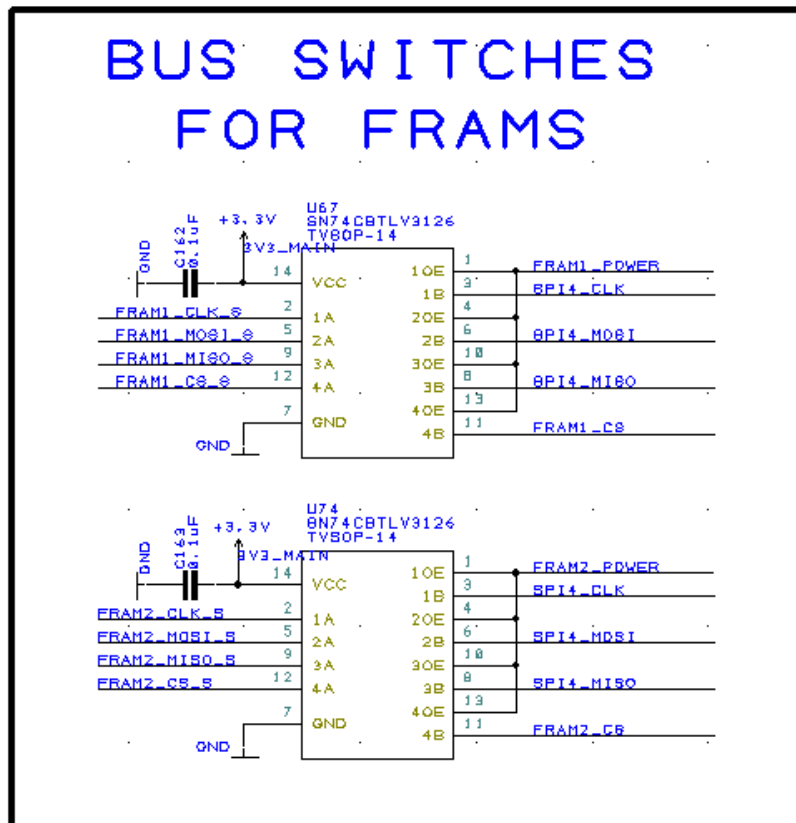


Figure 16: Top: two 4-bit bus switches for FRAMs. Bottom: a 4-bit bus switch external I²C buses.

BUS SWITCHES FOR MCU (PART 1)

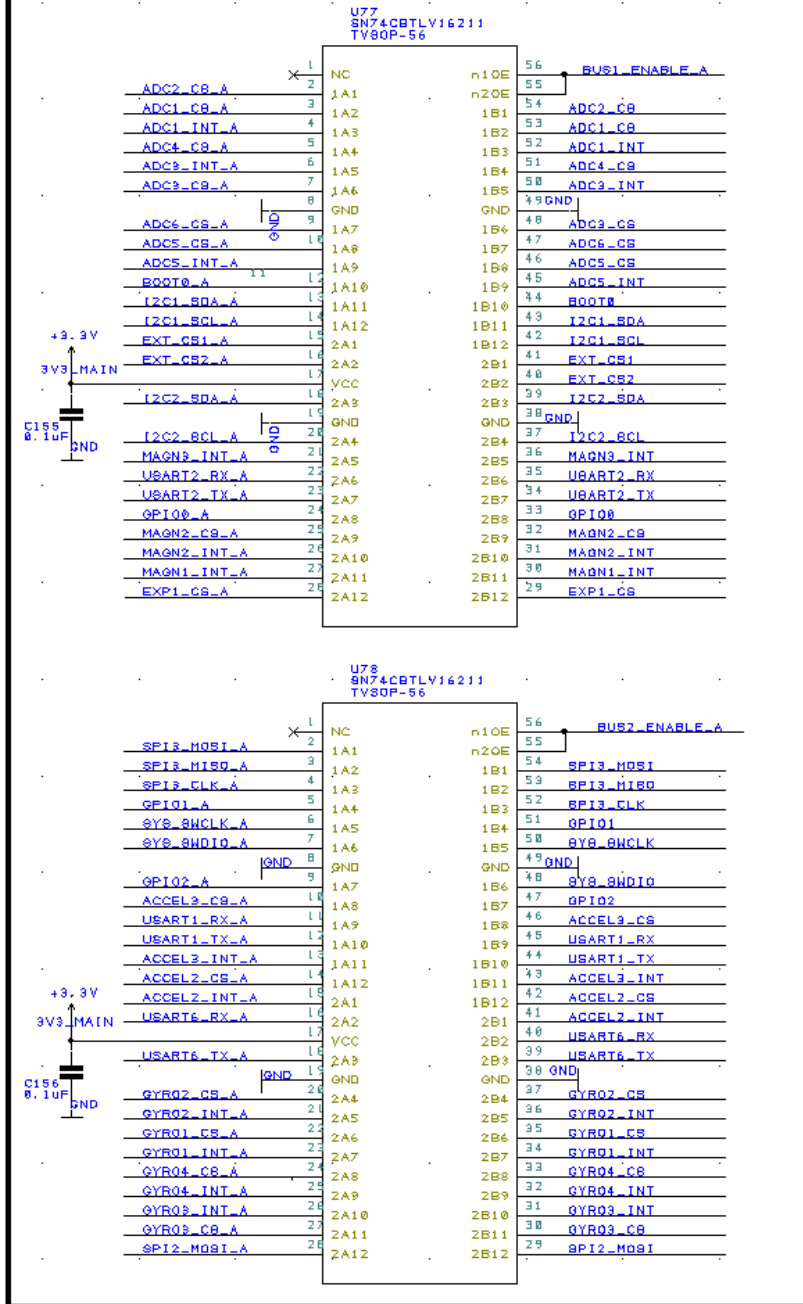
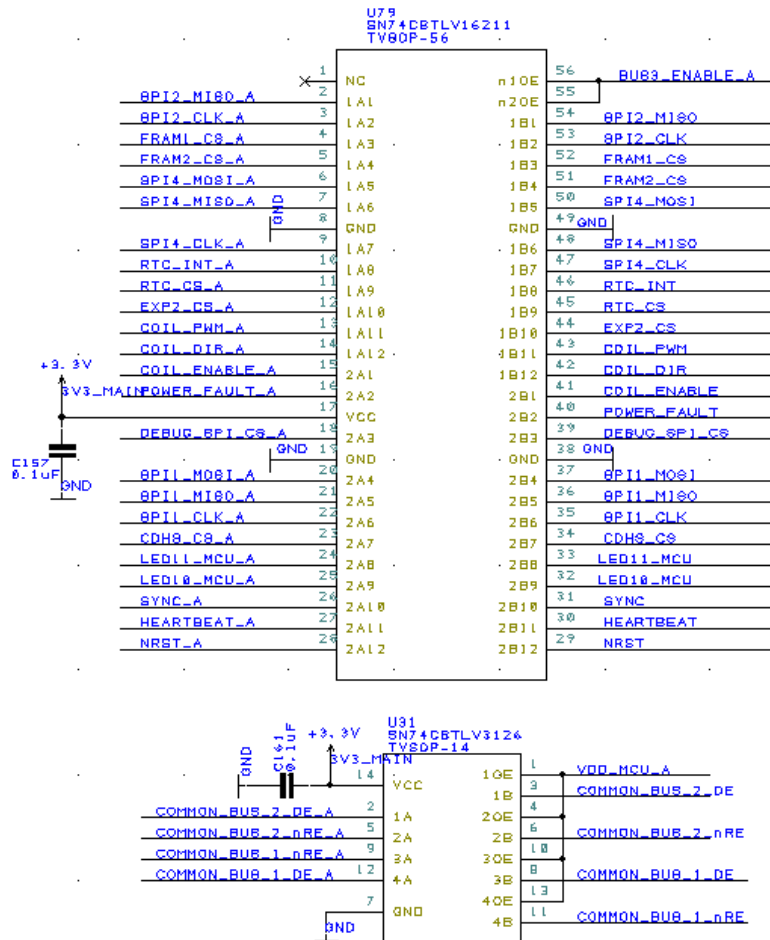


Figure 18: two 24-bit bus switches for MCU.

BUS SWITCHES FOR MCU (PART 1)



INVERTERS FOR MCU BUS SWITCHES

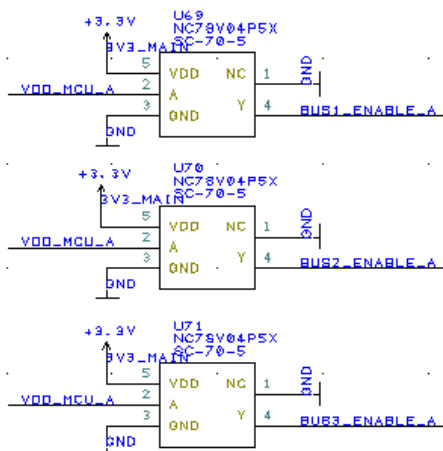


Figure 19: A 24-bit and a 4-bit bus switches for MCU.

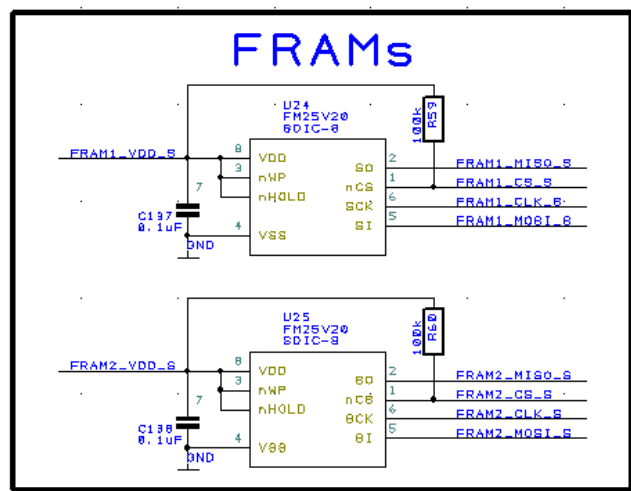
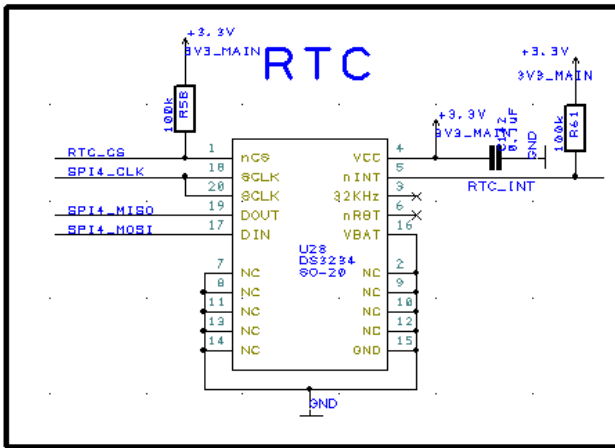
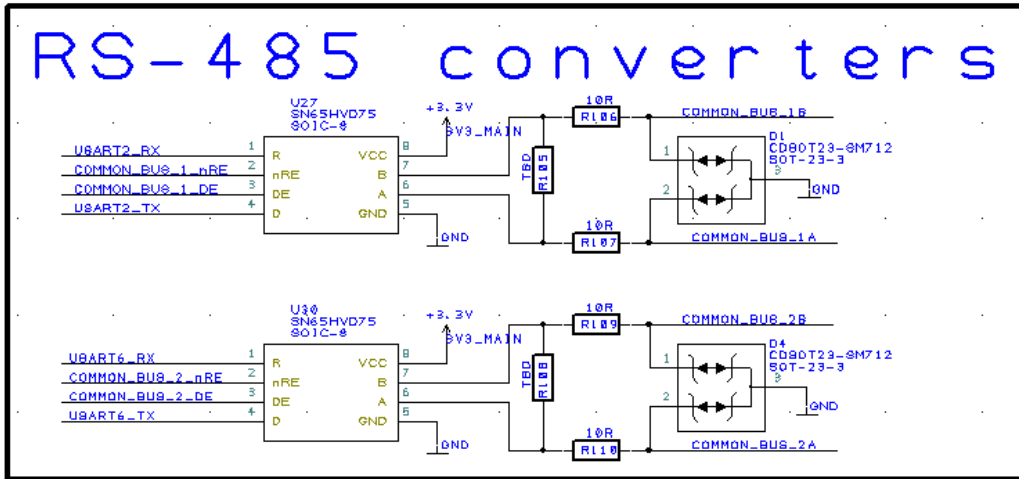


Figure 20: Top: two RS-485 converters. Bottom left: a real-time clock. Bottom right: two FRAMs.

Debugging group

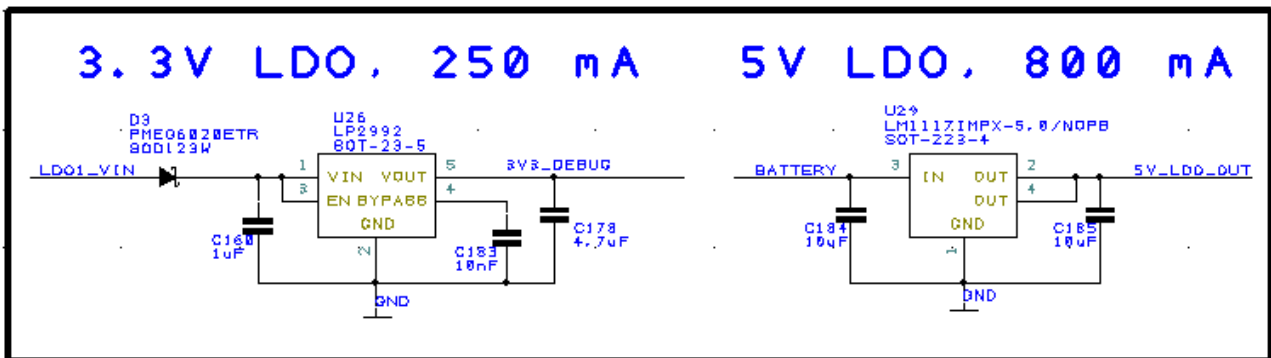


Figure 21: 3.3 V and 5 V LDOs.

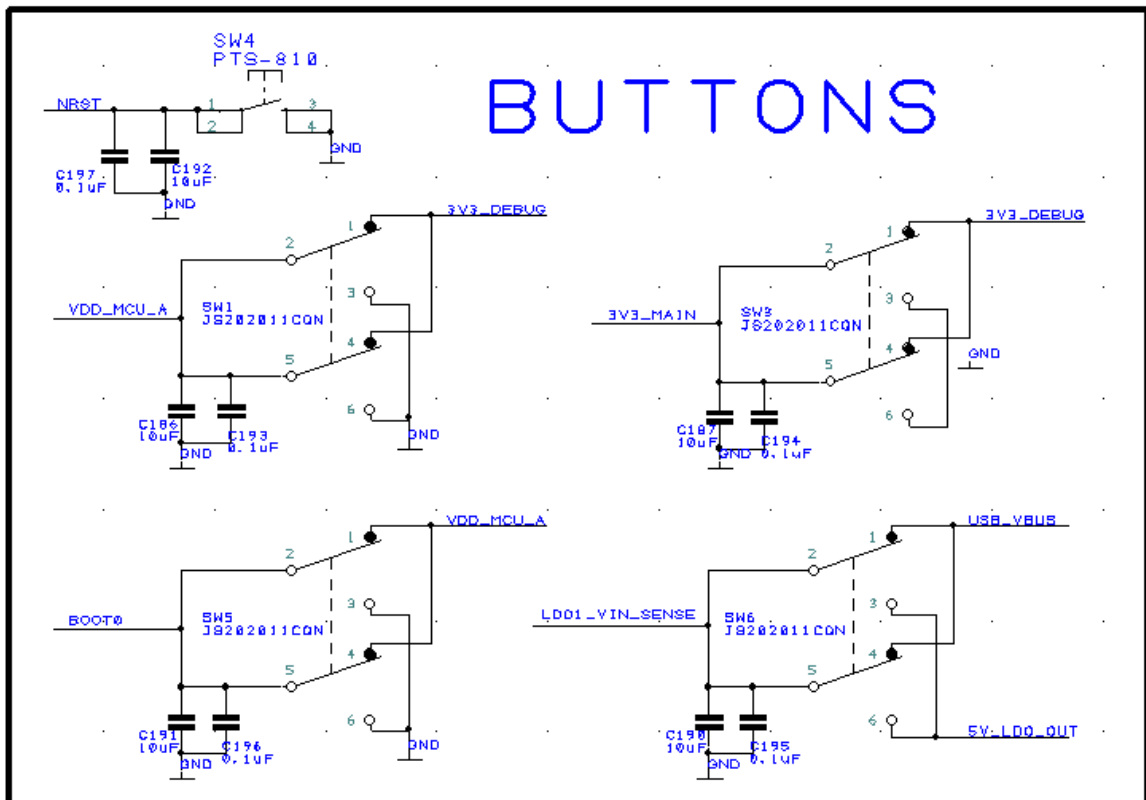
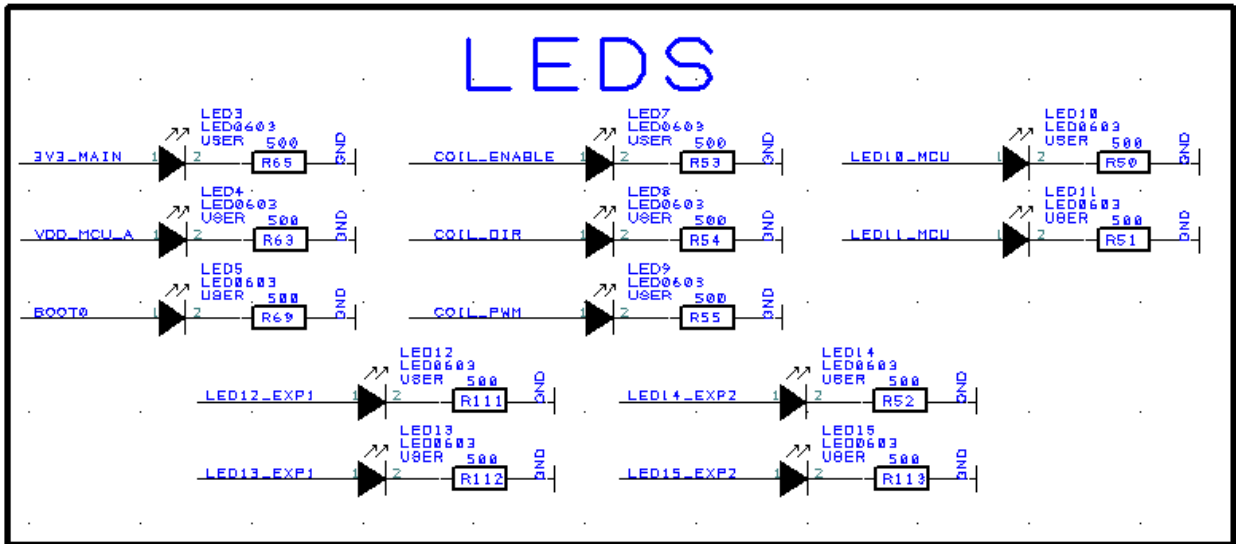
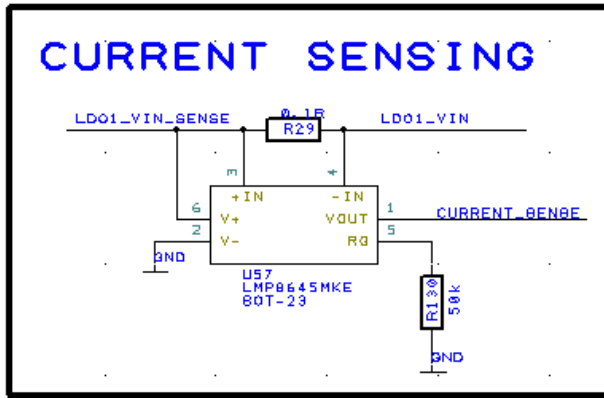


Figure 22: Top: current sensing amplifier. Middle: Indicator and debug LEDs. Bottom: buttons.

Connector group

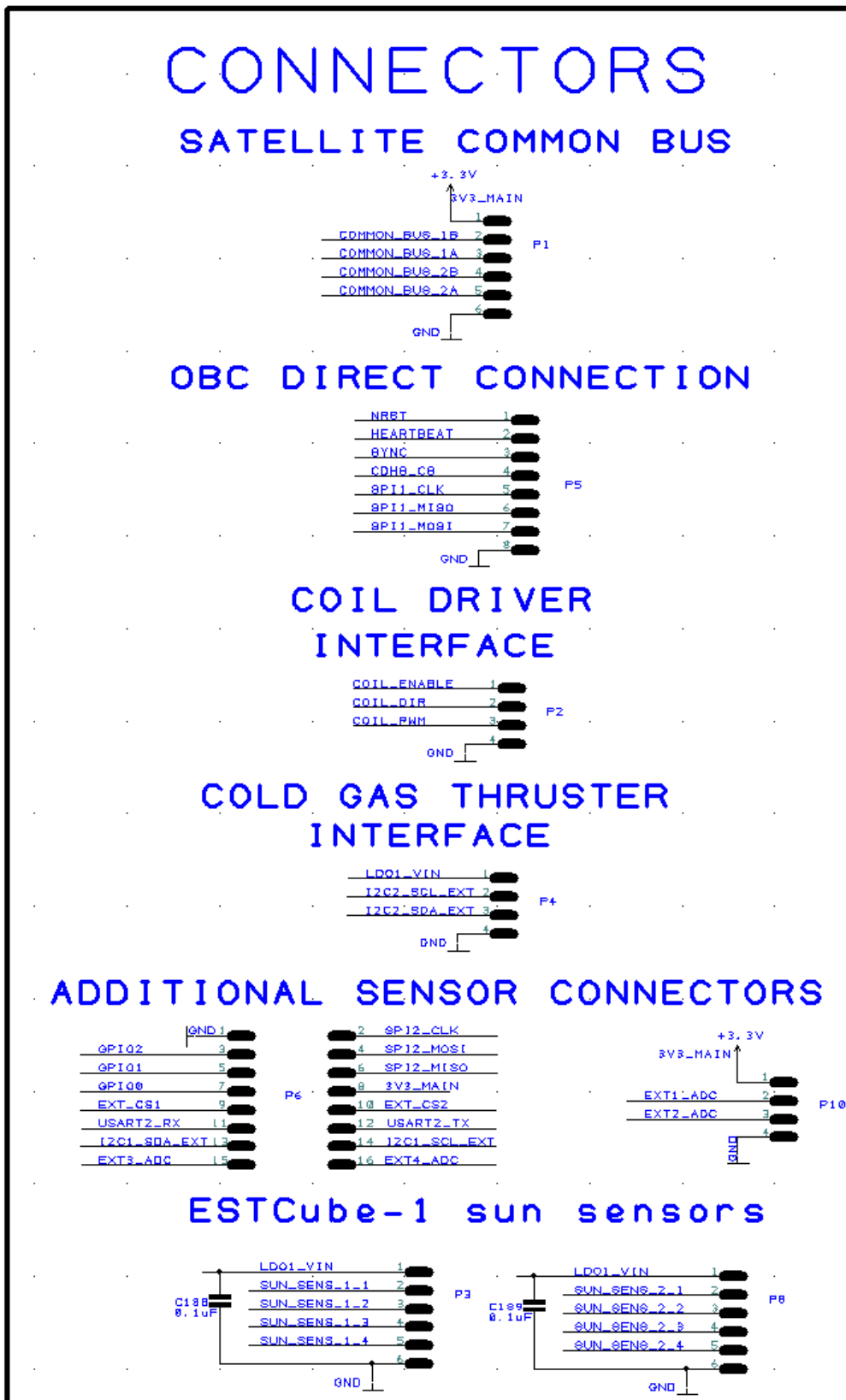
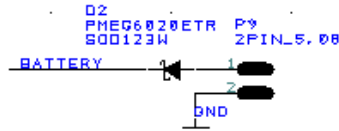


Figure 23: AOCS functionality connectors.

CONNECTORS

BATTERY CONNECTOR



DEBUG INTERFACE



USB and BATTERY 5V jumper

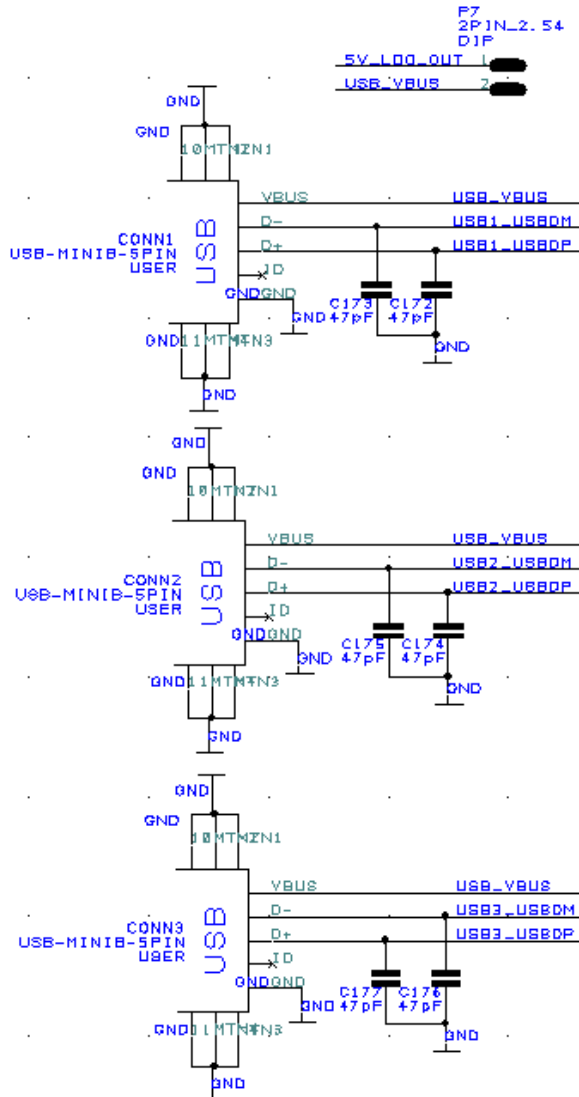


Figure 24: Power supply and debug connectors.

Appendix B – AOCS Prototype Board Layout (Full scale)

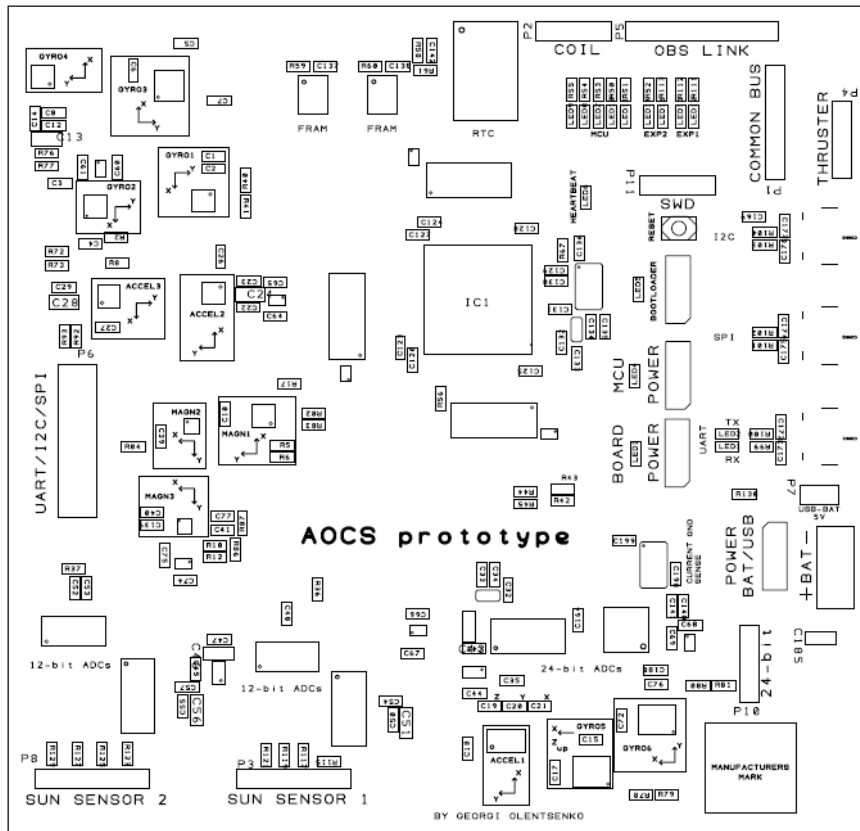


Figure 25: Top silkscreen.

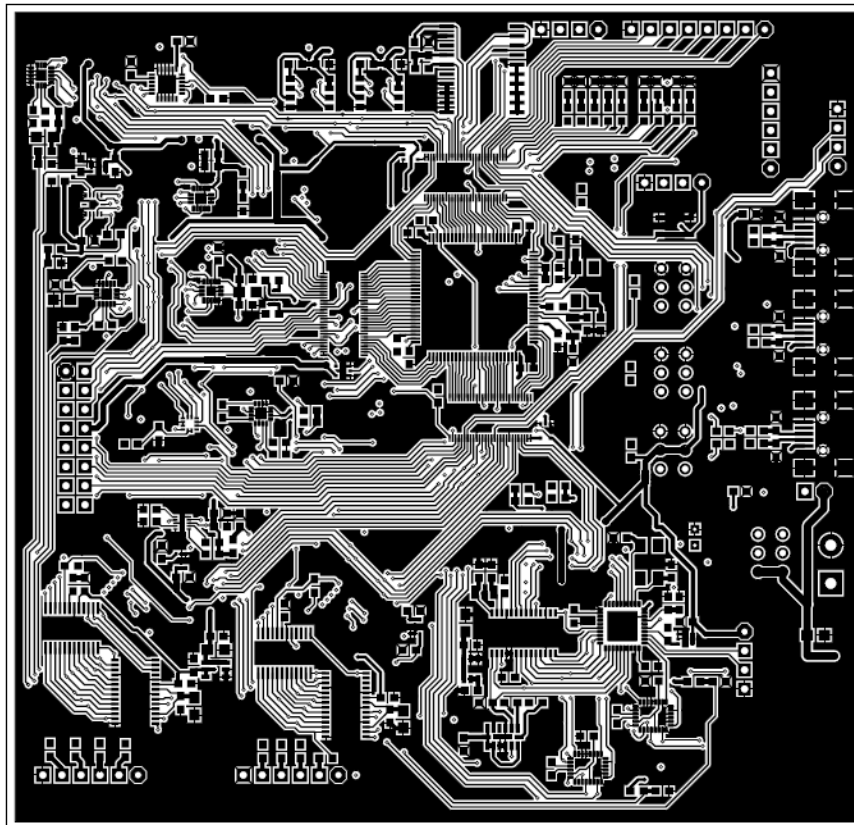


Figure 26: Top copper layer.

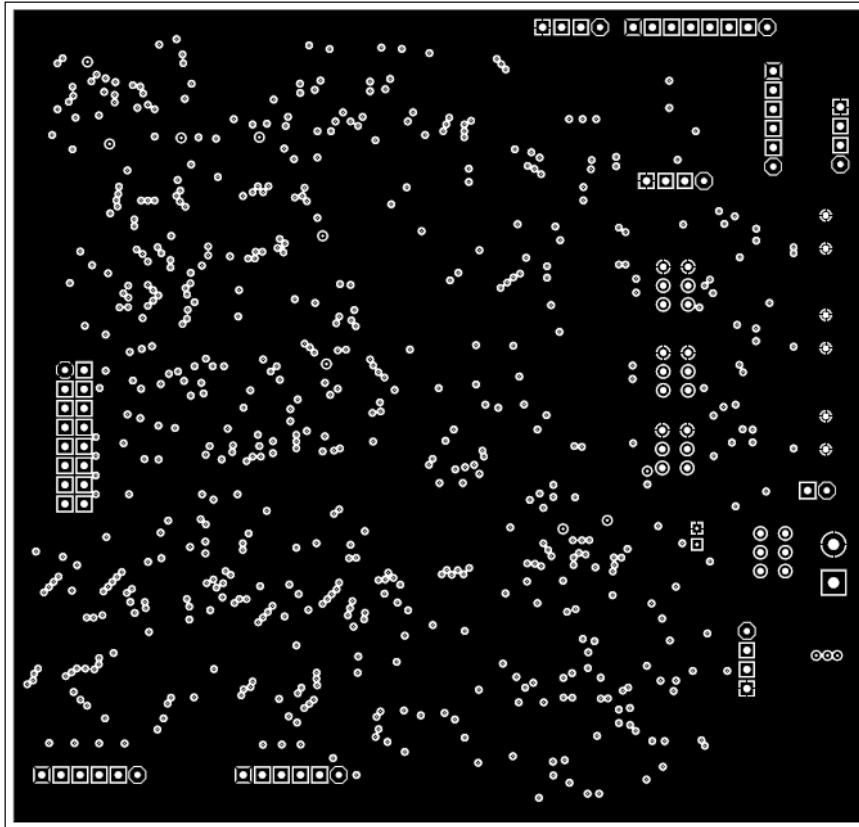


Figure 27: Inner 2 layer, ground plane.

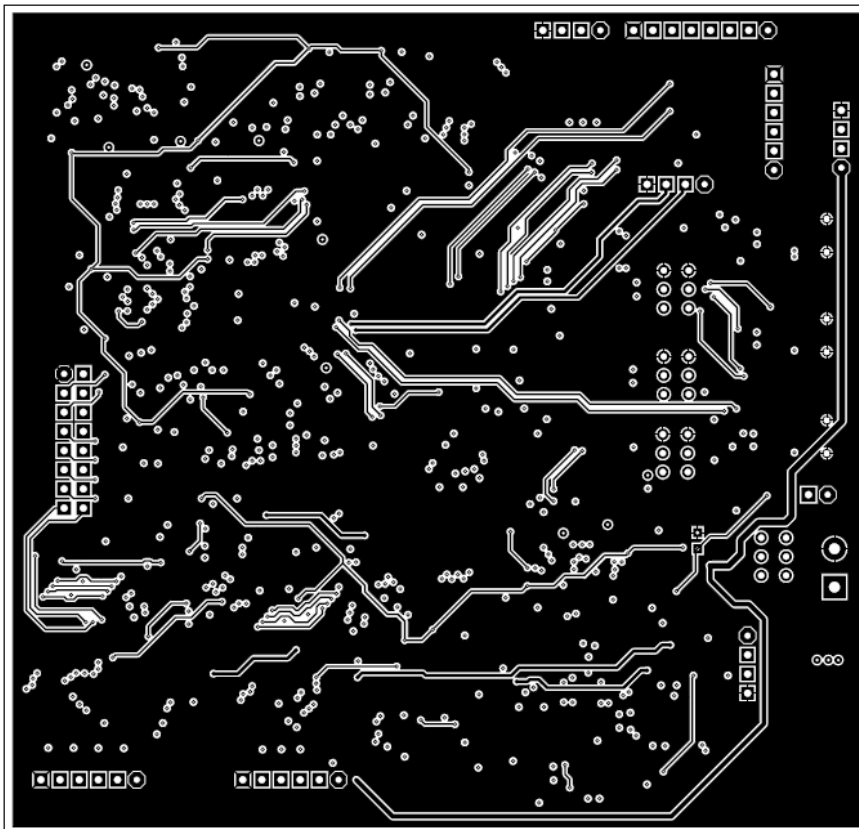


Figure 28: Inner 3 layer.

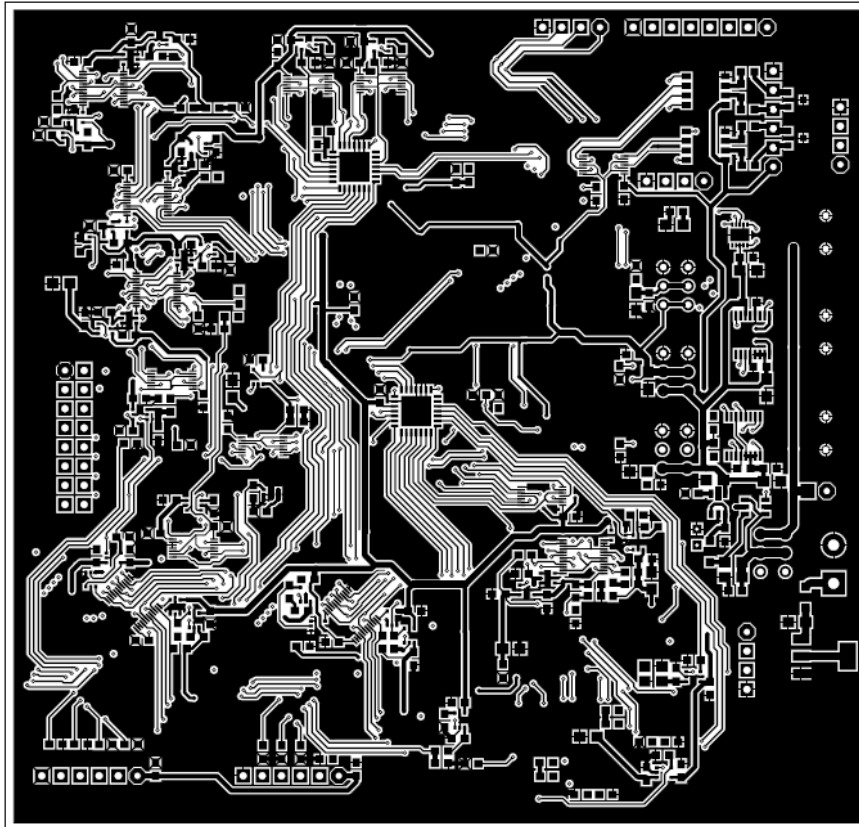


Figure 29: Bottom copper layer.

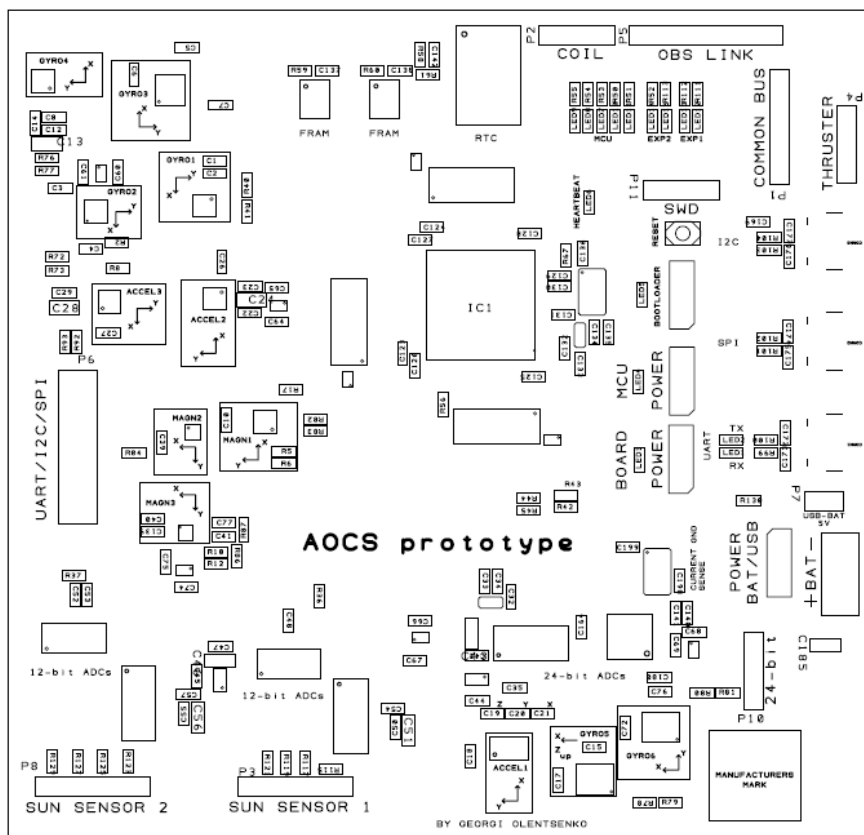


Figure 30: Bottom silkscreen.

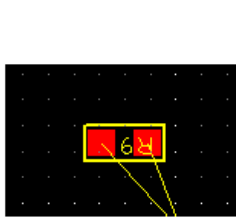
Appendix C – Prototype Board Bill of Materials

Amount	Name/Value	Package	Farnell ID	Mouser ID	Notes
1	MAX21000	LGA-16		700-MAX21000+	Digital gyroscope
1	BMG160	LGA-12		262-BMG160	Digital gyroscope
1	MPU-6000	QFN-24	1862383		Digital gyroscope and accelerometer
1	L3GD20H	LGA-16L		511-L3GD20HTR	Digital gyroscope
1	LPY403AL	LGA-28	1838539		Analog gyroscope
1	LPR403AL	LGA-28	1838534		Analog gyroscope
1	HMC5883L	LPCC-16	1971743		Digital magnetometer
1	LIS3MDL	VFLGA-12		511-LIS3MDLTR	Digital magnetometer
1	MAG3110	DFN-10		841-MAG3110FCR1	Digital magnetometer
1	KXR5	LGA-14		912-KXR5-2050	Analog accelerometer
1	FXC8700CQ	QFN-16		841-FXOS8700CQR1	Digital accelerometer and magnetometer
1	LSM303D	LGA-16		511-LSM303DTR	Digital accelerometer and magnetometer
6	LMT86QDCKQT Q1	SC-70-5	2361481		Temperature sensor
2	ADR3430ARJZ	SOT-23	1827386		3 V reference
1	AD7718	TSSOP-28		584-AD7718BRUZ	24-bit ADC
1	AD7173-8	LFCSP-40	2377349		24-bit ADC
2	MAX11633	QSOP-24		700-MAX11633EEG+	12-bit ADC
2	AD7490	TSSOP-28	9605231		12-bit ADC
20	TPS22941	SC-70-5	1778215		Load switch
2	MCP23S17	QFN-28		579-MCP23S17-E/ML	I/O expander
7	SN74CBTLV3126	TVSOP-14		595-SNCBTLV3126DGV R	4-bit bus switch
6	SN74CBTLV3384	TVSOP-24		595-SNCBTLV3384DGV R	10-bit bus switch
3	SN74CBTLV1621 1	TVSOP-56		595-SN74CB3T16211DG V	24-bit bus switch
15	NC7SC04P5X	SC-70-5	1467340		Inverter
1	STM32F401	LQFP-100	2393646		MCU

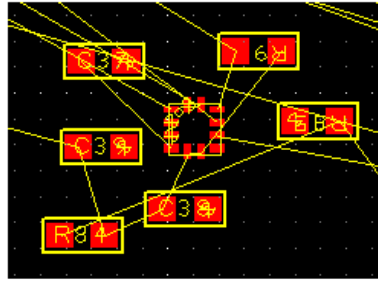
1	DS3234	SO-20	1593294		Real-time clock
2	FM25V20	SOIC-8		877-FM25V20-G	FRAM
2	SN65HVD75	SOIC-8	2127163		RS-485 converter
1	LP2992	SOT-23-5		926-2992AIM53.3/NOPB	3.3 V LDO
1	LM11171MPX-5.0/NOPB	SOT-223-4	2323593		5 V LDO
1	LMP8645MKE	SOT-23	1798345		Current sense amplifier
1	FT230XS-R	SSOP-16	2081321		USB to UART converter
1	FT220XD	SSOP-16	2081322		USB to SPI converter
1	FT200XD	DFN-10	2081320		USB to I ² C converter
2	ABMM2-16.000MHZ-E2-T		2101343		16 MHz crystal
2	FC-13F		1907465		32 kHz crystal
2	CDSOT23-SM712	SOT-23	1824869		TVS diode
2	PMEG6020ETR	SOD-123W	2311226		Diode
4	JS202011CQN		2320018		Slide switch
1	PTS810			611-PTS810SJM250SMT R	Tactile switch
4	Header pins		9731091		2.56 mm pitch 4 contacts 1 row
3	Header pins		9731113		2.56 mm pitch 6 contacts 1 row
1	Header pins		9731121		2.56 mm pitch 8 contacts 1 row
1	Header pins		2254695		2.56 mm pitch 16 contacts 2 rows
1	Header pins		9731075		2.56 mm pitch 2 contacts 1 row
1	Header pins		1926382		5.08 mm pitch 2 contacts 1 row

3	10033526-N3212MLF		2112367		Mini USB receptacle
8	18 pF	C0603	1759056		
6	47 pF	C0603	1759062		
6	1 nF	C0603	1759088		
1	2.2 nF	C0603	1759093		
3	4.7 nF	C0603	2310555		
5	10 nF	C0603	1759102		
95	100 nF	C0603	2280883		
2	220 nF	C0603	431199		
2	470 nF	C0603	2280913		
36	1 μ F	C0603	1759398		
2	2.2 μ F	C0603	2310406		
8	4.7 μ F	C0805	2310410		
17	10 μ F	C0805	2310738		
1	0.1 Ω	R0805	2008297		
4	10 Ω	R0603	2078895		
6	27 Ω	R0603	1697354		
2	150 Ω	R0603	2078902		
12	500 Ω	R0603	2331261		
2	3.3 k Ω	R0603	2078912		
6	4.7 k Ω	R0603	2078913		
2	10 k Ω	R0603	2078915		
13	33 k Ω	R0603	2078918		
1	50 k Ω	R0603	2331242		
8	68 k Ω	R0603	2078920		
46	100 k Ω	R0603	2078921		
22	1 M Ω	R0603	2078928		
2	TBD	R0603			
15	LED	0603	2322071		
Total of 451 components					

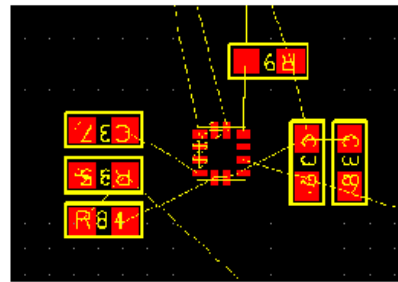
Appendix D – Board Layout Design Strategy



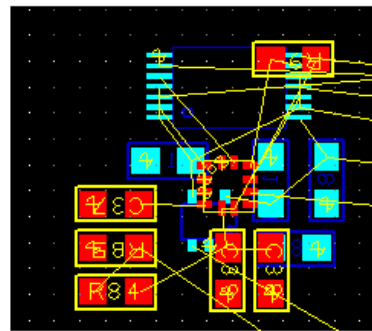
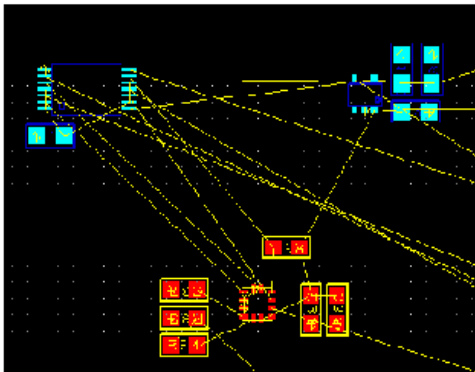
Initial state. Single components



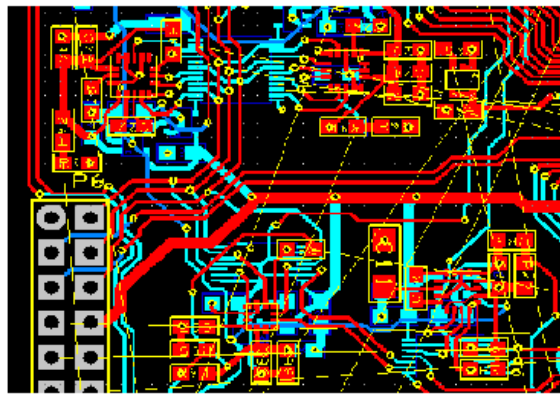
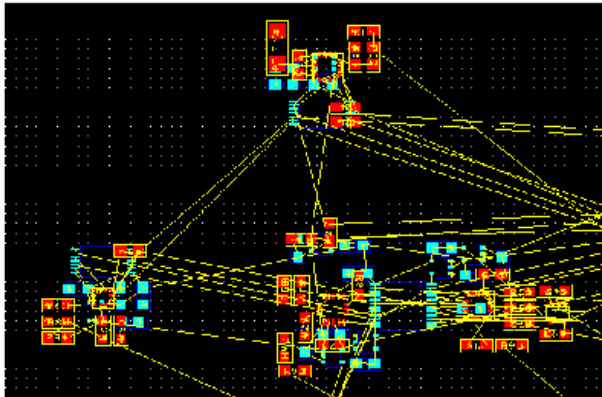
Step 1. Combine schematic groups



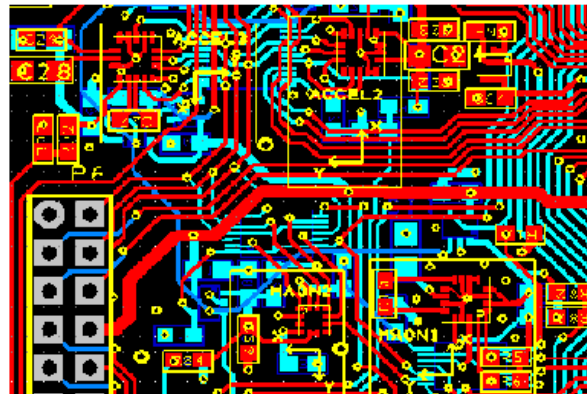
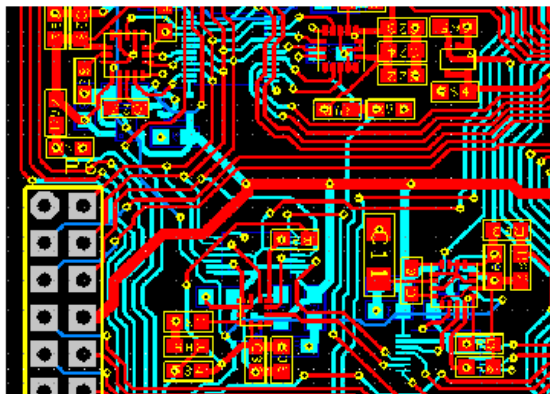
Step 2. Organize the group



Step 3. Combine the groups logically



Step 4. Combine the logical units, establishing the structure of the board and estimating the required space for signals



Step 5. Optimize the established structure and component placement

Appendix E – CD Contents

Table 6: Contents of the accompanying CD.

AOCS prototype design	Schematics and layout in DesignSpark and Gerber formats
georgi_thesis.pdf	A copy of the thesis
readme.txt	Description of the CD contents

Non-exclusive licence to reproduce thesis and make thesis public

I, Georgi Olentšenko (date of birth: 06.01.1990), herewith grant the University of Tartu a free permit (non-exclusive licence) to:

1.1. reproduce, for the purpose of preservation and making available to the public, including for addition to the DSpace digital archives until expiry of the term of validity of the copyright, and

1.2. make available to the public via the web environment of the University of Tartu, including via the DSpace digital archives until expiry of the term of validity of the copyright,

Prototype Design of ESTCube-2 Attitude and Orbit Control System supervised by Andris Slavinskis and Viljo Allik.

2. I am aware of the fact that the author retains these rights.

3. I certify that granting the non-exclusive licence does not infringe the intellectual property rights or rights arising from the Personal Data Protection Act.

Tartu, 27.05.2014